ELSEVIER

Marine Geology xx (2006) xxx–xxx

MARINE GEOLOGY
INTERNATIONAL JOURNAL OF MARINE GEOLOGY, GEOCHEMISTRY AND GEOPHYSICS

www.elsevier.com/locate/margeo

Late-stage estuary infilling controlled by limited accommodation space in the Hudson River

A.L. Slagle [a,*], W.B.F. Ryan [a], S.M. Carbotte [b], R. Bell [b], F.O. Nitsche [b], T. Kenna [b]

[a] *Department of Earth and Environmental Sciences and Lamont-Doherty Earth Observatory of Columbia University, P.O. Box 1000, Palisades, NY 10964-8000 USA*

[b] *Lamont-Doherty Earth Observatory of Columbia University, P.O. Box 1000, Palisades, NY 10964-8000 USA*

Received 31 March 2006; received in revised form 18 July 2006; accepted 28 July 2006

Abstract

High-resolution seismic data and sediment cores reveal the late Holocene subsurface stratigraphy of the broad Tappan Zee–Piermont region of the Hudson River Estuary. We identify a series of distinct, extensive horizons beneath the marginal flats, channel banks, and main channel in this area. Physical properties and lithology from sediment cores suggest that these horizons are surfaces of erosion or nondeposition. Radiocarbon dates indicate that they correspond with three distinct time horizons, with maximum ages of 3400, 2200, and 1600 yr BP. We also distinguish two sedimentary facies that occupy the marginal flats and channel banks. The deeper facies forms a deposit 2 km wide and 7 km long that accumulated at rates of 2–4 mm/yr in the vicinity of the Sparkill Creek prior to ~1700 yr BP, overlying and onlapping the 2200 yr BP seismic surface. Based on its internal geometry, morphology, and proximity to a tributary, we interpret this facies as a delta deposit. The shallower facies accumulated more slowly (1–2 mm/yr), overlying the delta deposit to the south and dominating the marginal flats to the north. Surface sediment samples and geophysical data reveal that the modern marginal flats are no longer actively depositional, but dominated by nondeposition or erosion. Limited accommodation space in the Hudson River Estuary may be the critical factor contributing to the observed sedimentary pattern, characterized by intervals of deposition punctuated by episodes of erosion. An estuarine system that has reached a state of morphological equilibrium will be sensitive to even small fluctuations in sea-level and climate conditions, which may account for the intervals of deposition and erosion we observe. Limited accommodation space and intermittent sediment deposition in the Hudson River Estuary may be due to its evolution from a fjord filled with glacial lake sediments, which distinguishes its infilling behavior from the classic drowned river valley estuary.

Keywords: estuarine sedimentation; accommodation space; Hudson River Estuary

1. Introduction

Estuarine sediment distribution is determined by the interplay of regional and local controls, including sea-level change, morphology and hydrodynamic conditions, sediment supply, and availability of accommodation space (Olsen et al., 1978; Dalrymple et al., 1992; Schlager, 1993; Boggs, 1995). General facies models predict broad sedimentary patterns in estuaries, based on the interaction between marine processes (waves and tides) and fluvial processes (e.g. Dalrymple et al., 1992), and associated with relative sea-level changes (e.g. Allen

* Corresponding author. Tel.: +1 845 365 8339; fax: +1 845 365 8156.
E-mail address: aslagle@ldeo.columbia.edu (A.L. Slagle).

0025-3227/$ - see front matter © 2006 Elsevier B.V. All rights reserved.
doi:10.1016/j.margeo.2006.07.009

and Posamentier, 1994; Zaitlin et al., 1994). There is a need to study estuaries such as the Hudson River Estuary, where other factors, such as inherited valley shape and accommodation space, may dominate (Heap and Nichol, 1997). For marine sedimentation, the concept of accommodation is defined as the space made available below some base level for potential sediment accumulation and preservation (Jervey, 1988). Previous studies document responses of some estuaries to limited or changing accommodation space, including slow, discontinuous flooding and deposition of marine–estuarine sediments (Heap and Nichol, 1997), lateral progradation rather than vertical accumulation (Dabrio et al., 2000; Hansen, 2004), and migration of the primary depocenter within the main estuary basin (Fletcher et al., 1992).

Early investigations of the Hudson River Estuary, primarily based on sediment samples, described the general patterns of morphology and sediment character of the estuary floor (Olsen et al., 1978; Coch and Bokuniewicz, 1986). Later studies identified regional variations in sediment distribution as well as specific areas of deposition and erosion along the estuary (Olsen et al., 1993; Feng et al., 1998). Observations concentrated on sediment transport and regional rates of accumulation associated with estuarine turbidity maxima have been carried out in recent years in the lower Hudson River Estuary (Geyer et al., 1998; Menon et al., 1998; Geyer et al., 2001; Pekar et al., 2004). With increased interest in the fate of contaminants, the lower estuary has also been a focal point for observations of anthropogenically-induced sediment accumulation (Ellsworth, 1986; Olsen et al., 1993; Abood and Metzger, 1996). Previous studies of the Hudson River Estuary have documented the nature of sedimentary facies on an estuary-wide scale (Weiss, 1974; Olsen et al., 1978; McHugh et al., 2004) and recent studies have focused on the development of facies in the lower estuary between New York City and Yonkers, NY (Traykovski et al., 2004; Klingbeil and Sommerfield, 2005).

In 1998, the New York State Department of Environmental Conservation initiated a project to map the bottom of the Hudson River Estuary between the New York Harbor and Troy, NY using geophysical surveys and bottom samples (Nitsche et al., 2005; Bell et al., 2006). In this paper, we use this high-resolution dataset to capture fine scale variations in sediment patterns that have not been resolved in generalized estuary models. We explore the evolution of the Hudson River Estuary by characterizing late Holocene sub-bottom stratigraphy and sedimentary facies in the broad, mesohaline Tappan Zee–Piermont area. We also develop an associated chronology for the region based on radiocarbon-dated material.

2. Regional setting

The ancestral Hudson River Valley was deepened by glacial erosion during the series of Pleistocene glacial and interglacial cycles (Newman et al., 1969; Coch and Bokuniewicz, 1986). The thalweg of the present valley, carved into Triassic sedimentary rock, sits between ~60 and 225 m below the estuary floor (Worzel and Drake, 1959; Newman et al., 1969). During the most recent interglacial period, meltwater was impounded between terminal moraines to form large proglacial lakes in the Hudson Valley. Following the most recent retreat of the Laurentide ice sheet from its maximum extent ~21,000 cal yr before present (BP), the terminal moraine at the Narrows was breached by the meltwater lakes, which then drained rapidly to the sea (Donnelly et al., 2005). As a result, the valley was first filled with glacial till and proglacial lacustrine clay, followed by fluvial sediment. As sea-level rose, marine water intruded further into the river system, eroding fluvial and glacial lake sediments and converting the lower portion of the system into an estuary. Estuarine conditions were established in the lower reaches of the Hudson River prior to 12,000 BP (Weiss, 1974) and a relatively thin layer of estuarine sediment continues to accumulate today.

The modern Hudson River Estuary is a tidally-dominated, partially mixed estuary. Its headwaters are in the southwestern part of the Adirondack Mountains and it flows south ~300 km to its mouth at New York Bay. The influence of the tides extends ~240 km upriver from the Battery to the dam near Troy, NY, with a tidal range between 1 and 2 m (Olsen et al., 1978). The focus of this study is a 20-km stretch of the lower estuary located between Piermont, NY and the Tappan Zee region (Fig. 1). In this area, the estuary opens up from the bedrock-bound reach along the island of Manhattan in New York City and Yonkers, NY to the broad bay of the Tappan Zee. In the southern half of the study area, the estuary is confined by the diabase of the Palisades Sill to the west and the metamorphic and igneous rocks of the Manhattan Prong to the east (Coch and Bokuniewicz, 1986; Isachsen et al., 2000). The northern half of the study area is also bound by the Manhattan Prong to the east, but the geology to the west consists of softer Newark Basin sediments. The Sparkill Creek enters the estuary from the west, through the Piermont Marsh (Fig. 1). The Tappan Zee Bridge and Piermont Pier are prominent anthropogenic structures that have occupied the study area for the last 50 and ~150 yr, respectively.

Please cite this article as: A.L. Slagle et al., Late-stage estuary infilling controlled by limited accommodation space in the Hudson River, Marine Geology (2006), doi:10.1016/j.margeo.2006.07.009.

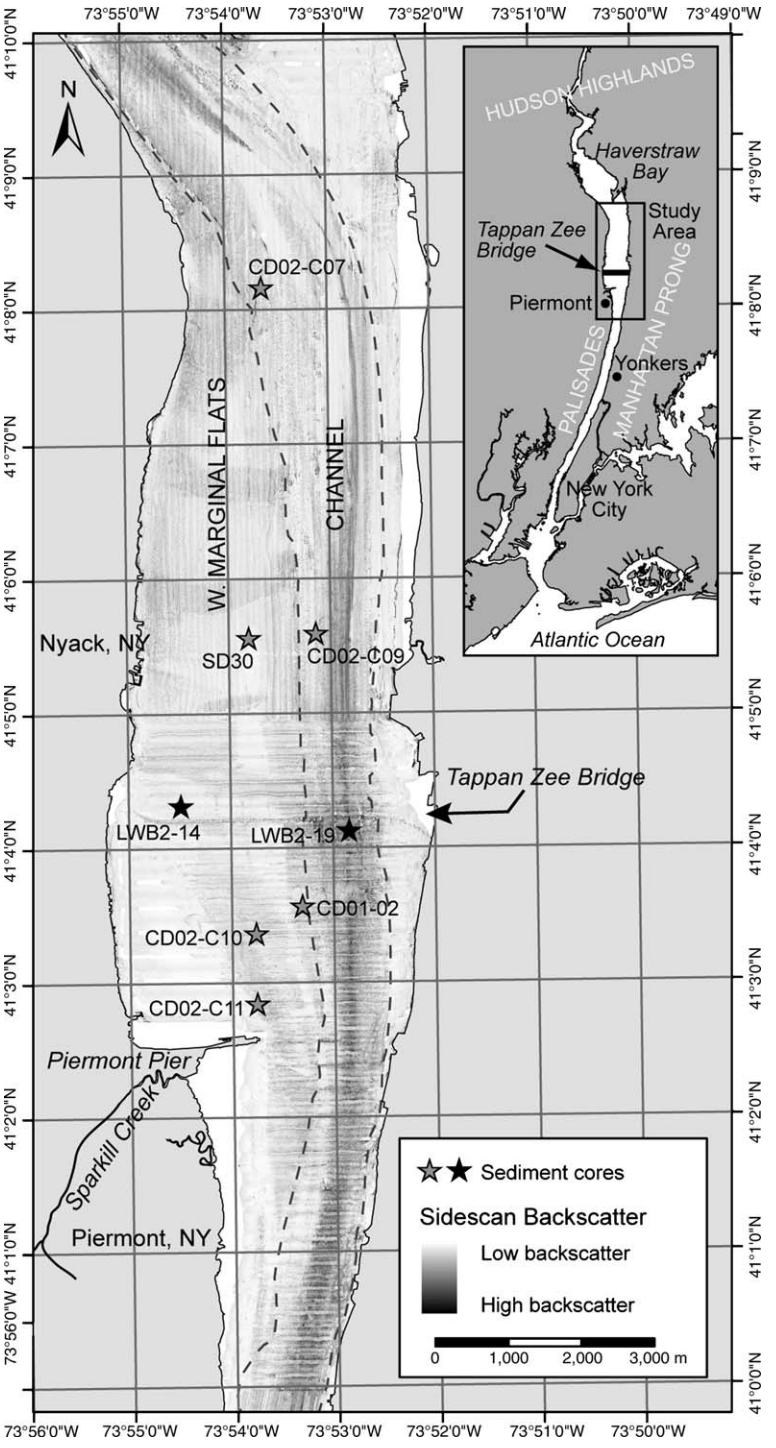

Fig. 1. Sidescan sonar mosaic of Tappan Zee–Piermont area of Hudson River Estuary. Dark pixels represent high backscatter and light pixels represent low backscatter. Gray stars indicate location of vibra-cores; black stars indicate gravity cores discussed in the text. Dashed lines show main channel. Inset shows location of study area along the Hudson River Estuary, with key geographic features referred to in the text.

In cross-section, the Tappan Zee–Piermont area is characterized by a ~15 m deep channel that occupies only a small part of the total width of the estuary (Figs. 1 and 3). The channel is slightly asymmetrical, with steeper channel banks to the east. Relatively shallow marginal flats (4–5 m deep)

Please cite this article as: A.L. Slagle et al., Late-stage estuary infilling controlled by limited accommodation space in the Hudson River, Marine Geology (2006), doi:10.1016/j.margeo.2006.07.009.

border the channel and extend to the estuary banks. The marginal flats to the west of the channel are between 1 and 2 km wide, while the eastern flats are typically less than 1 km wide. Fossil oyster beds extend in flow-perpendicular bands across the estuary in this area. They are exposed on the estuary floor as well as buried by sediment. Radiocarbon-dated sediment cores indicate that oysters flourished during two time periods, ~500–2400 and ~5600–6100 cal yr BP, and these fluctuations may reflect climatic changes associated with warm–cool cycles during the Holocene (Carbotte et al., 2004).

3. Methods

3.1. Sidescan sonar and sub-bottom profiling

Acoustic data collection for the Hudson River Benthic Mapping project, launched by the New York State Department of Environmental Conservation in 1998, included coverage of all areas greater than 4 m water depth. Sidescan sonar data were collected using a dual frequency EdgeTech DF-1000 (100 and 384 kHz) sidescan sonar system, towed 1.5 m below the water surface (Fig. 1). Simultaneous with sidescan sonar operations, sub-bottom reflection data were collected using an EdgeTech 4–24 sub-bottom sonar and XSTAR acquisition system. The sonar was operated with a sweep frequency of 4 to 16 kHz for optimal resolution, providing a practical vertical resolution of 5–10 cm. The sub-bottom sonar was towed 0.5 m below the water surface, with tow speeds ranging from 4 to 5.5 knots. A constant correction for tow fish depth was applied, computed from the average travel time difference between the water-bottom return and first water-bottom multiple. Data were collected on an orthogonal grid, with 80 m between north–south lines and 160 m between east–west lines (Fig. 2). All data were collected using differential GPS and shotpoints were layback corrected to account for the distance between towed sensors and the GPS antenna.

The ESRI ArcMap® Geographic Information System (GIS) software provided the spatial basis for interpretation and map creation. GeoFrame software provided the capability to identify and map seismic horizons and correlate them with sediment cores. To associate horizons with sediment cores, we converted two-way travel time to depth down-core by assuming a constant velocity of 1500 m/s in estuarine sediment. Using this estimate, 0.005 s of two-way travel time is equivalent to 3.75 m of sediment.

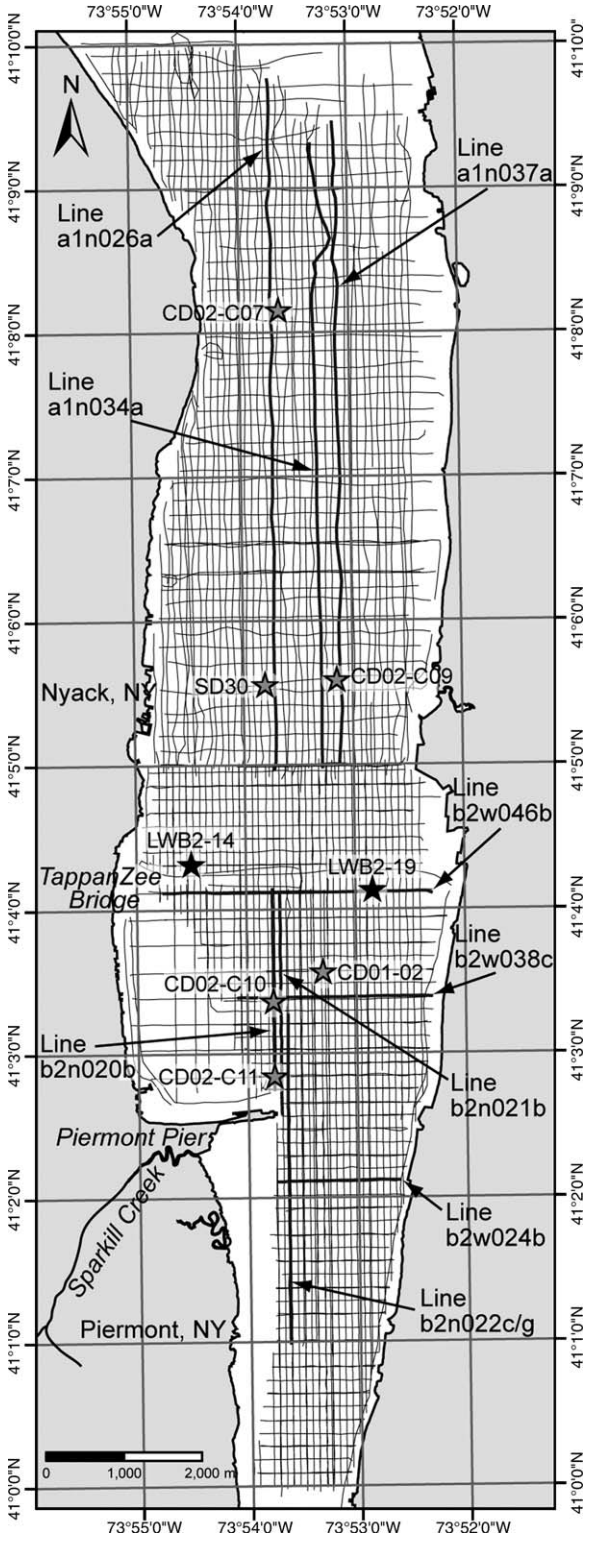

Fig. 2. Sidescan sonar and chirp sub-bottom track coverage in Tappan Zee–Piermont area. Labeled tracks correspond to chirp profiles shown in (Figs. 4, 5, and 9). Core locations are indicated by gray stars (vibracores) and black stars (gravity cores).

Please cite this article as: A.L. Slagle et al., Late-stage estuary infilling controlled by limited accommodation space in the Hudson River, Marine Geology (2006), doi:10.1016/j.margeo.2006.07.009.

Table 1
Sediment core locations in the Tappan Zee–Piermont area

Core ID	Type	Latitude (°N)	Longitude (°W)	Water depth[a] (m)	Core length (m)	^{137}Cs in core top[b]
CD02-C07	Vibracore	41.136029	73.894052	8.08	5.975	nd
CD02-C09	Vibracore	41.093252	73.885787	9.91	5.80	nd
CD02-C10	Vibracore	41.056151	73.896050	3.63	6.07	nd
CD02-C11	Vibracore	41.047479	73.895992	5.39	6.08	nd
LWB2-14	Gravity	41.071900	73.908233	2.70	1.51	nd
LWB2-19	Gravity	41.068767	73.880733	13.50	0.785	nd
CD01-02	Vibracore	41.059567	73.888460	6.01	5.24	–
SD30	Vibracore	41.092708	73.896757	4.36	9.31	–
CD02-C08[c]	Vibracore	41.136279	73.882804	9.14	5.94	nd
CD02-C12[c]	Vibracore	41.003401	73.895389	7.86	5.86	yes (50.2 [6.6])
CD02-C30[c]	Vibracore	41.026738	73.889051	7.10	8.19	yes (51.2 [13.1])

[a] Water depth below mean sea level referenced to NAVD88.
[b] Presence of ^{137}Cs considered positive if any amount was measured in excess of two times the one-sigma error; *nd* indicates that ^{137}Cs was not detected;– indicates that ^{137}Cs was not measured. Activity, shown in parentheses, was decay-corrected to the core collection date (CD02-C12 5/31/2002; CD02-C30 6/3/2002); reported units are pCi/wet kg; one-sigma error shown in brackets.
[c] Cores are shown only with ^{137}Cs data in Fig. 6a.

3.2. Sediment sampling

A set of short gravity cores (<2 m) and longer vibracores (8–10 m) provide lithological information and material for radiocarbon dating as well as ground truth information for the geophysical datasets (Table 1). Cores are curated and stored at the U.S. National Science Foundation-supported Core Repository at Lamont-Doherty Earth Observatory. Sediment physical properties, including compressional (*P*-wave) velocity, gamma ray attenuation (bulk density), and magnetic susceptibility, were measured using a GEOTEK Multi-Sensor Core Logger. Following geophysical analysis, cores were split longitudinally, measured, photographed, and described. Cores were examined as soon as possible after splitting to minimize color alteration and matched with standard color chips on a Munsell® soil color chart. In addition to color, each core was described by noting dominant grain size, sedimentary structures, biological components, and the nature of stratigraphic contacts.

Following description, selected cores were sampled for radiocarbon analysis and later for loss-on-ignition (LOI; Dean, 1974). Sediment sub-samples (2–3 cc) from three vibra-cores were washed through a 63 μm sieve, dried, and weighed to measure percent coarse fraction. Core-top samples from seven vibra-cores were measured for presence of ^{137}Cs by gamma spectrometry. Undried surface sediments were placed directly on the gamma detector (either of two lithium-drifted germanium planar detectors or a high-purity germanium well detector). Corrections to the measured ^{137}Cs counts included background, counting efficiency, geometry, branching ratio, and wet sample mass to obtain ^{137}Cs activity per wet kilogram. All ^{137}Cs activities were then decay corrected to the core collection date.

3.3. Radiocarbon dating

Shell material (from oysters, small bivalves, and gastropods) and wood were sampled for radiocarbon analysis. A study by Colman et al. (2002) indicated that biogenic carbonate from clam and oyster shells provides some of the most reliable material for radiocarbon dating in the Chesapeake Bay estuary. Samples were analyzed by accelerator mass spectrometry at the Lawrence Livermore National Laboratory's Center for Accelerator Mass Spectrometry. Ages were calculated according to the methods of Stuiver and Polach (1977), using assumed values of δ^{13}C (Table 2). The radiocarbon ages were converted to calendar ages relative to 1950 using the calibration program CALIB 4.3 (Stuiver and Reimer, 1993).

Because biogenic carbonate in the Hudson River Estuary is precipitated from estuarine water, that pool determines the initial radiocarbon content of the shells. Open ocean water typically has a ^{14}C deficit relative to the atmosphere, constituting a reservoir effect of ~400 yr (Stuiver and Reimer, 1993). The reservoir correction for the Hudson River Estuary varies from this standard marine reservoir age because of mixing with river water, which is contaminated by older terrestrial carbon. Analyses of three shell samples from the Hudson River Estuary between Piermont and Haverstraw Bay, collected alive before atmospheric nuclear bomb testing, indicate that reservoir ranges from 800 to 1200 ^{14}C years (Peteet and Rubenstone, personal

Please cite this article as: A.L. Slagle et al., Late-stage estuary infilling controlled by limited accommodation space in the Hudson River, Marine Geology (2006), doi:10.1016/j.margeo.2006.07.009.

Table 2
Radiocarbon ages in the Tappan Zee–Piermont study area

Core ID	Sample depth (cm)	Material [a]	$\delta^{13}O$ (per mil) [b]	Age (^{14}C yr) [c]	Error (yr) [d]	Age with Hudson reservoir correction (min, max) (cal. yr B.P.) [e]	Age with marine reservoir correction (min, max) (cal. yr B.P.) [f]	Age with terrestrial correction (min, max) (cal yr B.P) [g]
CD02-07	262	Bivalve	−2.5	3185	35	2208 (2131, 2342)	2961 (2866, 3074)	–
	329	CV	−2.5	3510	35	2738 (2494, 2752)	3379 (3322, 3461)	–
CD02-09	204	CV	−2.5	2655	35	1578 (1528, 1707)	2329 (2289, 2394)	–
CD02-10	291	CV	−2.5	2955	45	1963 (1834, 2060)	2733 (2683, 2788)	–
	488	CV	−2.5	3375	35	2396 (2349, 2710)	3243 (3151, 3332)	–
CD02-11	69	Gastropod	−2.5	3000	40	1995 (1899, 2120)	2753 (2710, 2842)	–
	276	CV	−2.5	3500	40	2735 (2474, 2752)	3371 (3306, 3461)	–
CD01-02	85	Wood	−25	2260	45	–	–	2215 (2149, 2349)
	135	Wood	−25	2390	40	–	–	2355 (2340, 2707)
	135	Charcoal	−25	2060	40	–	–	1999 (1902, 2145)
	504	Gastropod or bivalve	0	2805	40	1818 (1634, 1880)	2538 (2369, 2700)	–

[a] Material: CV, *Crassostrea virginica*.
[b] $\delta^{13}O$ values assumed according to Stuiver and Polach (1977).
[c] Quoted age is in radiocarbon years using the Libby half life of 5568 yr, following the conventions of Stuiver and Polach (ibid.).
[d] One sigma.
[e] Radiocarbon ages are calibrated to calendar years using CALIB 4.3 (Stuiver and Reimer, 1993), after applying a reservoir correction of 950 yr obtained from pre-bomb shells within the study area (J. Rubenstone and D. Peteet, unpublished data); Two sigma error is reported.
[f] Radiocarbon ages are calibrated to calendar years using a global marine dataset in CALIB 4.3 (Stuiver and Reimer, 1993); Two sigma error is reported.
[g] Radiocarbon ages are calibrated to calendar years using a terrestrial dataset within CALIB 4.3 (Stuiver and Reimer, 1993); Two sigma error is reported.

communication). Samples in this study were calibrated using a reservoir correction determined by averaging the reservoir values of the two pre-bomb shells located in closest proximity to our sediment cores (an average reservoir correction of 950 ^{14}C years, Table 2). In a detailed study of the Chesapeake Bay Estuary, benthic organisms such as bivalves tend to be in contact with denser, more saline water, and a standard marine correction alone was used successfully to calibrate biogenic carbonate (e.g. Cronin et al., 2000; Colman et al., 2002).

All radiocarbon ages in this study are reported in calendar years before present (BP). In Table 2, we provide ages calibrated with the Hudson reservoir correction as well as with the standard marine correction of Stuiver and Reimer (1993). Given the uncertainties inherent in the reservoir correction, our ages are rounded to the nearest hundred except where individual dated shells are cited.

4. Results

Our seismic reflection profile data reveal a series of regionally extensive horizons across various morphological environments throughout the Tappan Zee–Piermont area. The sediment fill in the study area falls into two distinct depositional facies based on reflection terminations, acoustic character, and lithology.

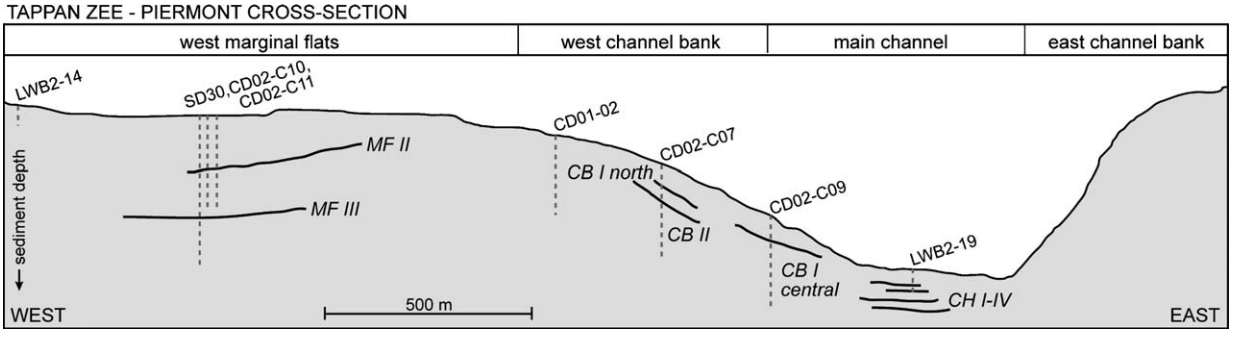

Fig. 3. Schematic cross-section of the Tappan Zee–Piermont area. Cores, projected onto the east to west profile, are indicated by dashed lines. Heavy lines show the relative sub-bottom positions of regional horizons beneath the marginal flats (MF horizons), west channel banks (CB horizons), and main channel (CH horizons).

Please cite this article as: A.L. Slagle et al., Late-stage estuary infilling controlled by limited accommodation space in the Hudson River, Marine Geology (2006), doi:10.1016/j.margeo.2006.07.009.

4.1. Regional horizons

Integration of sub-bottom data and sediment cores allows us to map and characterize a series of seismic horizons that cover broad areas in this stretch of the estuary. These horizons are bright, relatively continuous reflections, typically flat-lying or gently dipping. In map view, they extend 3 to 6 km in the north–south direction, but are relatively narrow across the estuary in the east–west direction (≤ 1 km). The most extensive horizons are imaged beneath the shallow marginal flats west of the main channel ("MF" horizons). Prominent horizons are also mapped beneath the western channel banks, dominantly in the northern region of the study area ("CB" horizons), and a series of horizons of more limited mapped extent is found beneath the channel in the southern portion of the study area ("CH" horizons). A schematic east to west cross-section of the Tappan Zee–Piermont area is shown in Fig. 3, illustrating the horizons in their relative locations and the sediment cores that sample them.

At the majority of sites where cores sample the horizons, they coincide with layers of shells and shell fragments. The horizons are also typically accompanied by shifts in *P*-wave velocity, gamma density and/or magnetic susceptibility in sediment cores (Fig. 4). Radiocarbon data provide some age control for the regional horizons, while seismic stratigraphy constrains the relative age relationships. The samples used to constrain horizon ages were isolated shells, shells collected from mixed shell and fragment layers, or dense wood layers, which could be transported or reworked material. Consequently, the resulting ages are regarded as maximum limits for the seismic horizons.

Horizon MF II is located in the west marginal flats and imaged as a southward- and westward-dipping reflection with an irregular surface (Fig. 5a–b, e). In lateral extent, horizon MF II stretches 5 km in the estuary-parallel direction and < 1 km across the marginal flats (Fig. 6c). At its southern margin, horizon MF II dips beneath the depth of seismic penetration (approx. 4 m) and may extend farther south than mapped. An oyster just above the horizon in core CD02-C10 is dated at 1963 BP (Fig. 7), so horizon MF II is interpreted to be older than this age. Using a sedimentation rate calculated from radiocarbon dates from core CD02-C11 (Fig. 8), we extrapolate to the depth of horizon MF II and assign an age of 2100 BP. To the north, MF II is transected by previously studied vibracore SD30 (Carbotte et al., 2004; Pekar et al., 2004; see Fig. 1 for location). Based on changes in sediment properties and radiocarbon data from SD30, MF II was interpreted as an erosional unconformity or hiatus in deposition of age ~1750 to 2500 BP (Carbotte et al., 2004), which spans our estimated age for horizon MF II to the south. Shallow oyster beds in this part of the estuary dip northward onto horizon MF II (Figs. 5a and 9a; Carbotte et al., 2004). If horizon MF II is an erosional surface, it may have provided a hard substrate suitable for oyster colonization in the estuary.

Horizon MF III is a bright, horizontal reflection mapped in the west marginal flats at ~3 m depth, beneath horizon MF II (Fig. 5b). In lateral extent, horizon MF III stretches for at least 6 km along-estuary and < 1 km across the marginal flats (Fig. 6d). It is mapped to ~1 km south of the Tappan Zee Bridge, where it dips below the depth of seismic penetration. It may be more extensive to the north but shallow relict oyster beds, which are acoustically impenetrable, hinder mapping this deep horizon farther north with certainty. Horizon MF III is also transected by core SD30 and a radiocarbon date from this core places the horizon with a maximum age of 3425 BP (Carbotte et al., 2004).

Horizons CB I central and CB I north lie at ~2 to 2.5 m depth within the west channel banks and are imaged as bright, irregular reflections (Fig. 5c–d). In lateral extent, horizons CB I central and CB I north stretch 5–6 km parallel to the estuary and < 1 km across the estuary (Fig. 6b). A shell from core CD02-C09 at the depth of the horizon has been dated at 1578 BP. Horizons CB I central and CB I north may be contemporaneous; eroded oyster beds in the channel bank sediments mask acoustic imaging beneath them and prevent a clear correlation. There is no dated material at the depth of horizon CB I north, but stratigraphic relations require it to be younger than a deeper channel bank horizon, dated with a maximum age of 2208 BP (horizon CB II, below; Fig. 5d).

The deepest horizon within the west channel banks is *horizon CB II*, mapped over approximately the same area as CB I north (Fig. 6c). Horizon CB II is imaged at 2.5 m depth in the channel terrace and west channel bank in the northern part of the study area and is characterized by a bright, smooth reflection (Fig. 5d). Horizon CB II is flat-lying and sits below a series of eroded oyster beds along the channel edge. A bivalve shell at the depth of the horizon in core CD02-C07 has been dated at 2208 BP. Taking into account age uncertainties associated with sparse control points and reservoir correction, horizon CB II may be contemporaneous with horizon MF II in the west marginal flats (Fig. 6c).

A series of four horizons have been mapped beneath the modern channel, *horizons CH I* (youngest) through *CH IV* (oldest). They are imaged as bright reflections with rough surfaces and may be indicative of older

Please cite this article as: A.L. Slagle et al., Late-stage estuary infilling controlled by limited accommodation space in the Hudson River, Marine Geology (2006), doi:10.1016/j.margeo.2006.07.009.

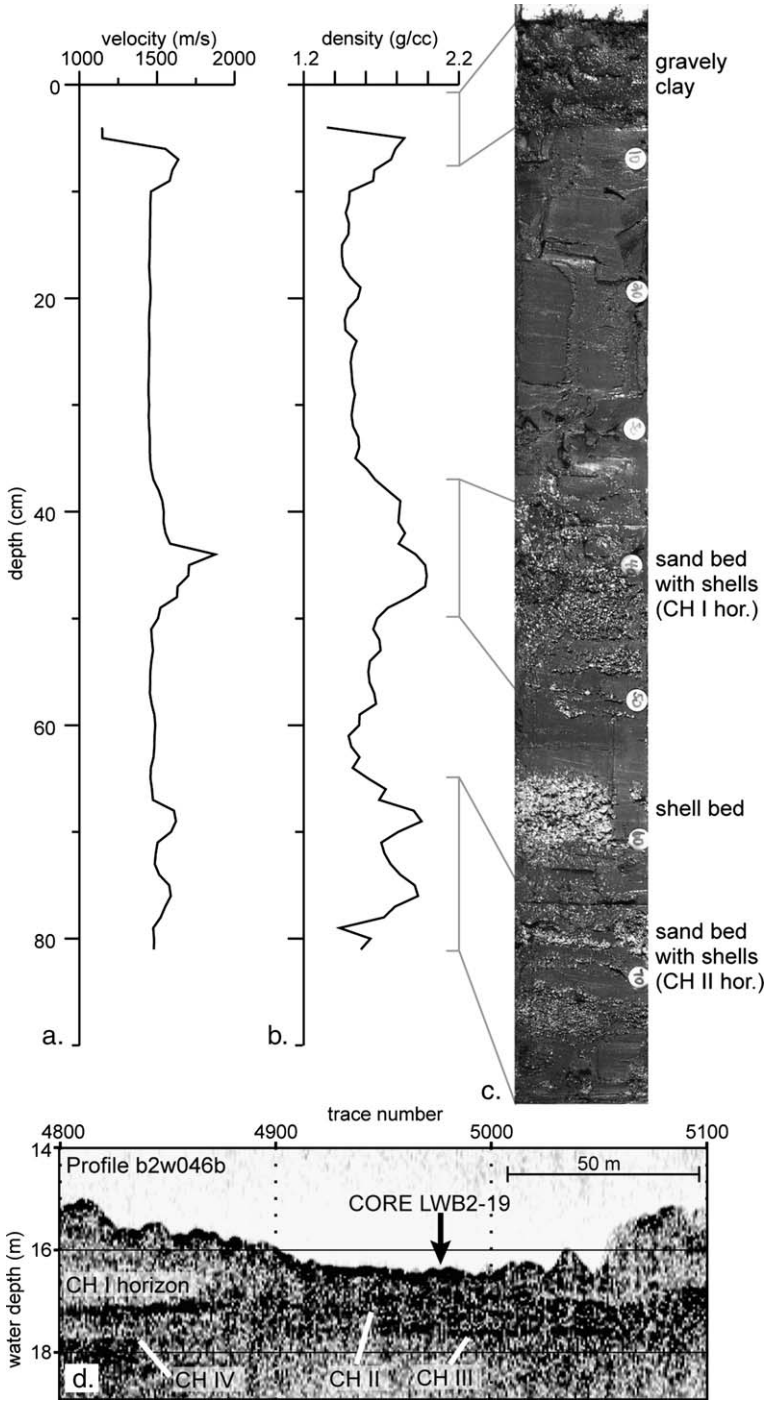

Fig. 4. Peaks in *P*-wave velocity (a) and gamma density (b) profiles correspond to sandy, shelly layers shown in a photograph of core LWB2-19 (c), located within the channel. These changes are associated with bright reflections beneath the channel imaged in seismic profiles, horizons CH I, II, III, and IV (d). Two-way travel time has been converted to depth assuming a sediment velocity of 1500 m/s.

channel floor topography (Fig. 4d and Fig. 5e). The CH horizons extend beneath the modern channel bank with a gentle dip to the west and appear near-horizontal under the channel. In lateral extent, the CH horizons stretch <4 km along-estuary and <1 km across the estuary, occupying a smaller area than the marginal flats and channel banks horizons. These horizons dip below the depth of seismic penetration to both north and south and

Please cite this article as: A.L. Slagle et al., Late-stage estuary infilling controlled by limited accommodation space in the Hudson River, Marine Geology (2006), doi:10.1016/j.margeo.2006.07.009.

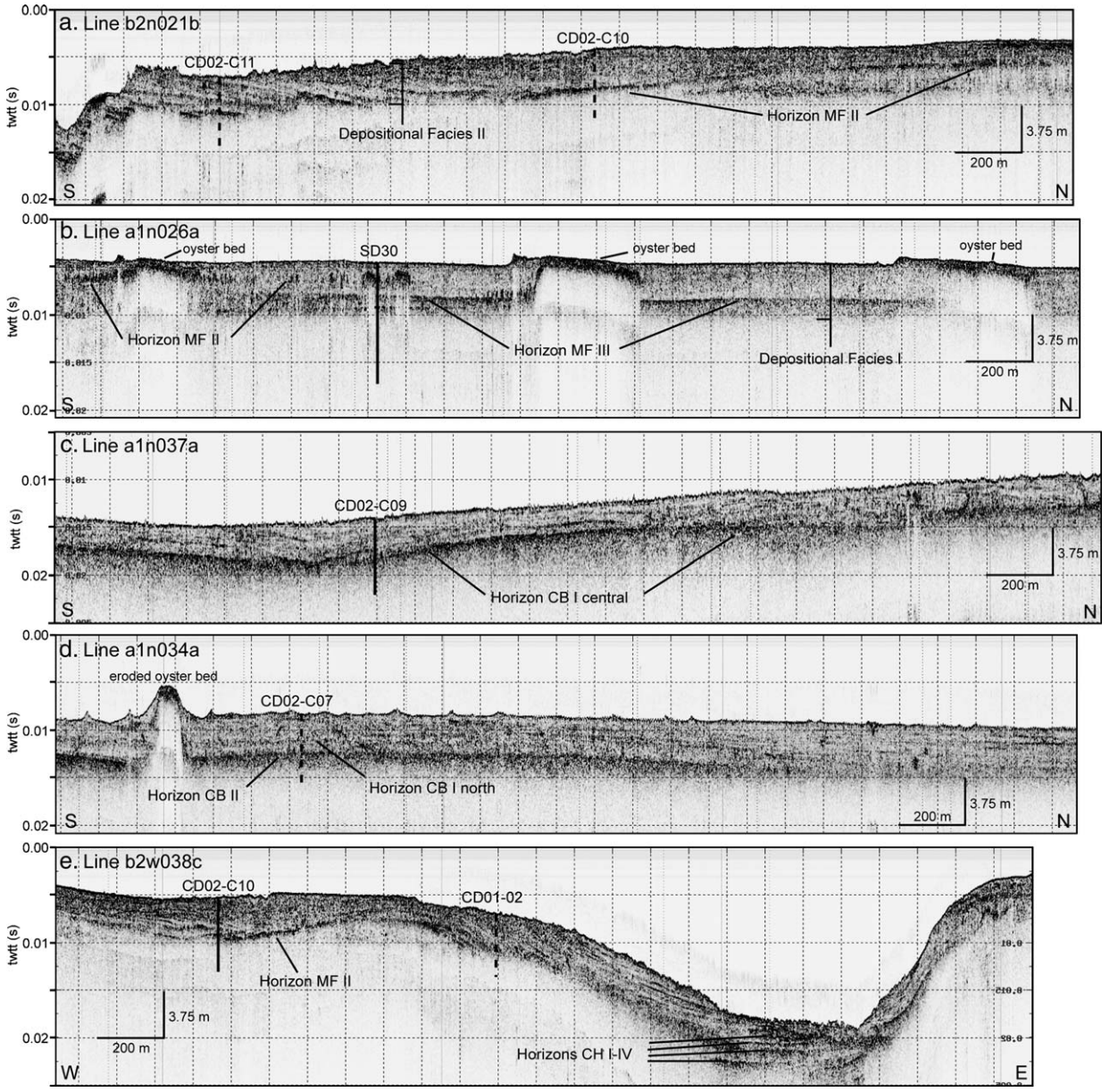

Fig. 5. Seismic profiles illustrating regional horizons. Core locations and lengths are shown on each profile. Dashed lines indicate cores that are projected onto profiles, from 100 to 700 m away. Note the dipping reflections of depositional Facies II (a) and the acoustic transparency of Facies I (b). Oyster beds are imaged as bright, acoustically impenetrable reflections.

may be more extensive than mapped. Although we have no dates to constrain their absolute ages, the geometry of channel bank horizons CB I north, CB I central, and CB II suggests that channel bank sediments are prograding across successive CH horizons.

4.2. Depositional facies (I–II)

In addition to seismic horizons, sub-bottom data allow us to distinguish discrete units in the estuarine sediment fill, dominantly within the marginal flats of the study area. The two primary facies have distinctive acoustic characteristics and reflection geometry. Sediment cores provide ground truth information for these depositional facies and allow us to characterize their lithology.

4.2.1. Facies I

Depositional facies I is mapped beneath and north of the Tappan Zee Bridge, occupying the entire width

Please cite this article as: A.L. Slagle et al., Late-stage estuary infilling controlled by limited accommodation space in the Hudson River, Marine Geology (2006), doi:10.1016/j.margeo.2006.07.009.

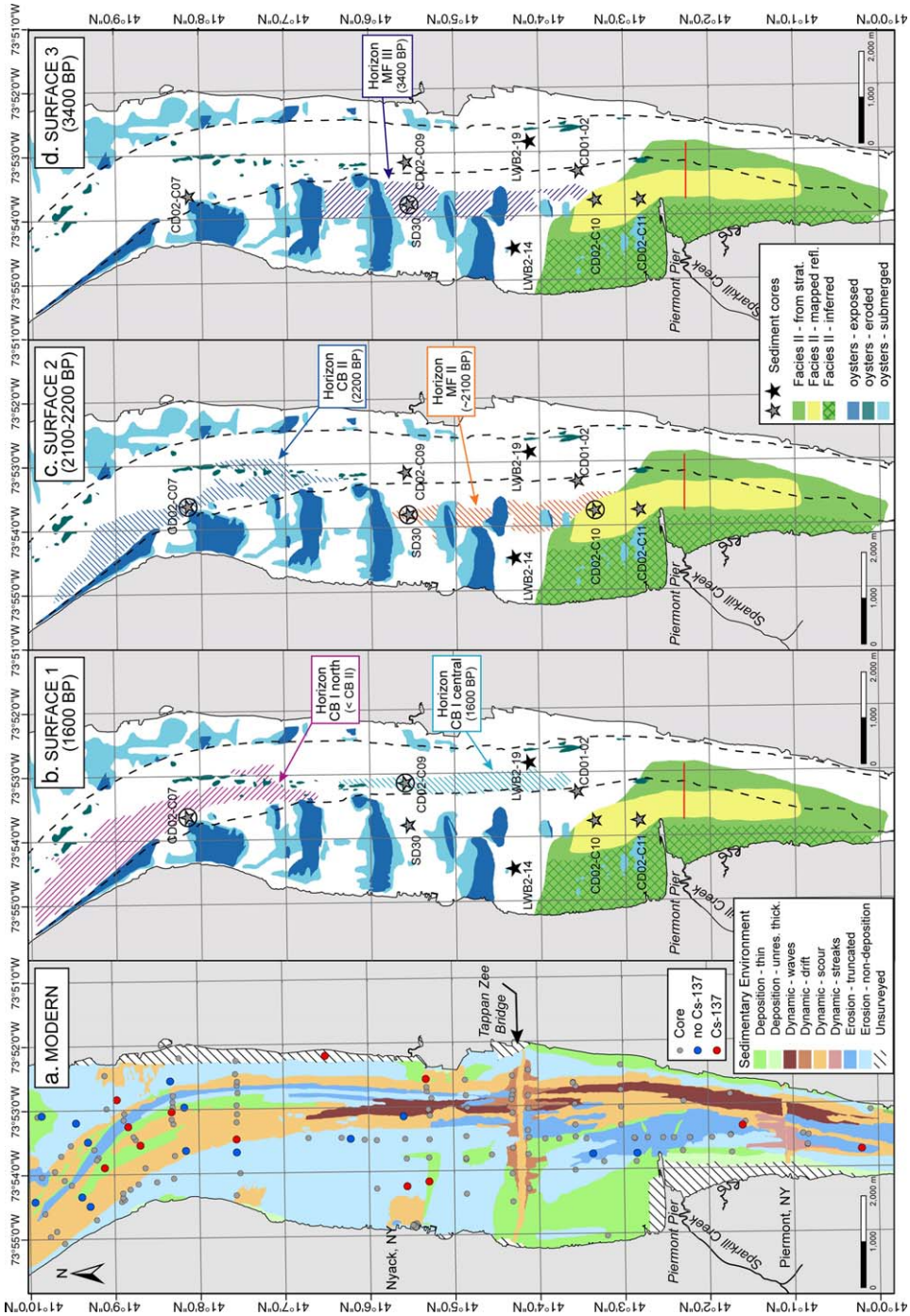

Fig. 6. Modern sedimentary environment of the Tappan Zee–Piermont area (a). Integration of acoustic data, bathymetry, and sediment samples for ground truth reveal distinct sedimentary environments for the modern estuary floor. Green colors indicate *deposition*; blue shades indicate *erosion*; brown color shows sediment *waves*; and tan and gold colors show dynamic environments, characterized by erosion and deposition. Dynamic *scour* indicates areas where strong currents scour the bottom and move sediment along, while *drifts* and *streaks* form behind flow obstructions. For detailed description of sedimentary environment interpretation, see Bell et al. (2004) and Nitsche et al. (2004). Colored circles show sediment cores where ^{137}Cs was measured in core top samples. Locations and presence/absence of ^{137}Cs for samples from this study are shown in Table 1. All additional ^{137}Cs samples from McHugh et al. (2004; Supplemental Material). Features mapped from sub-bottom data in the Tappan Zee–Piermont area (b-d). Sparkill Creek Delta Deposit (Facies II) is shown in green and yellow. Solid red line indicates latitude of the inflection point in delta geometry. Surface 1 (b) is interpreted as a surface of erosion or nondeposition from 1600 BP and is expressed by regional horizons CB I north and CB I central. Surface 2 (b) is expressed by horizons CB II and MF II and is interpreted to be ~ 2100–2200 BP. Surface 2 divides the delta deposit into two units (F IIA and F IIB), the younger of which onlaps the erosion surface (see Figs. 5a and 9a). Surface 3 (c) is the oldest surface mapped and is expressed by MF III, with an interpreted age of ~ 3400 BP. Key sediment cores are indicated by stars; circled stars identify cores that provided age information for each horizon. Mapped oyster beds are shown in blue colors. The main channel is outlined by dashed lines.

Please cite this article as: A.L. Slagle et al., Late-stage estuary infilling controlled by limited accommodation space in the Hudson River, Marine Geology (2006), doi:10.1016/j.margeo.2006.07.009.

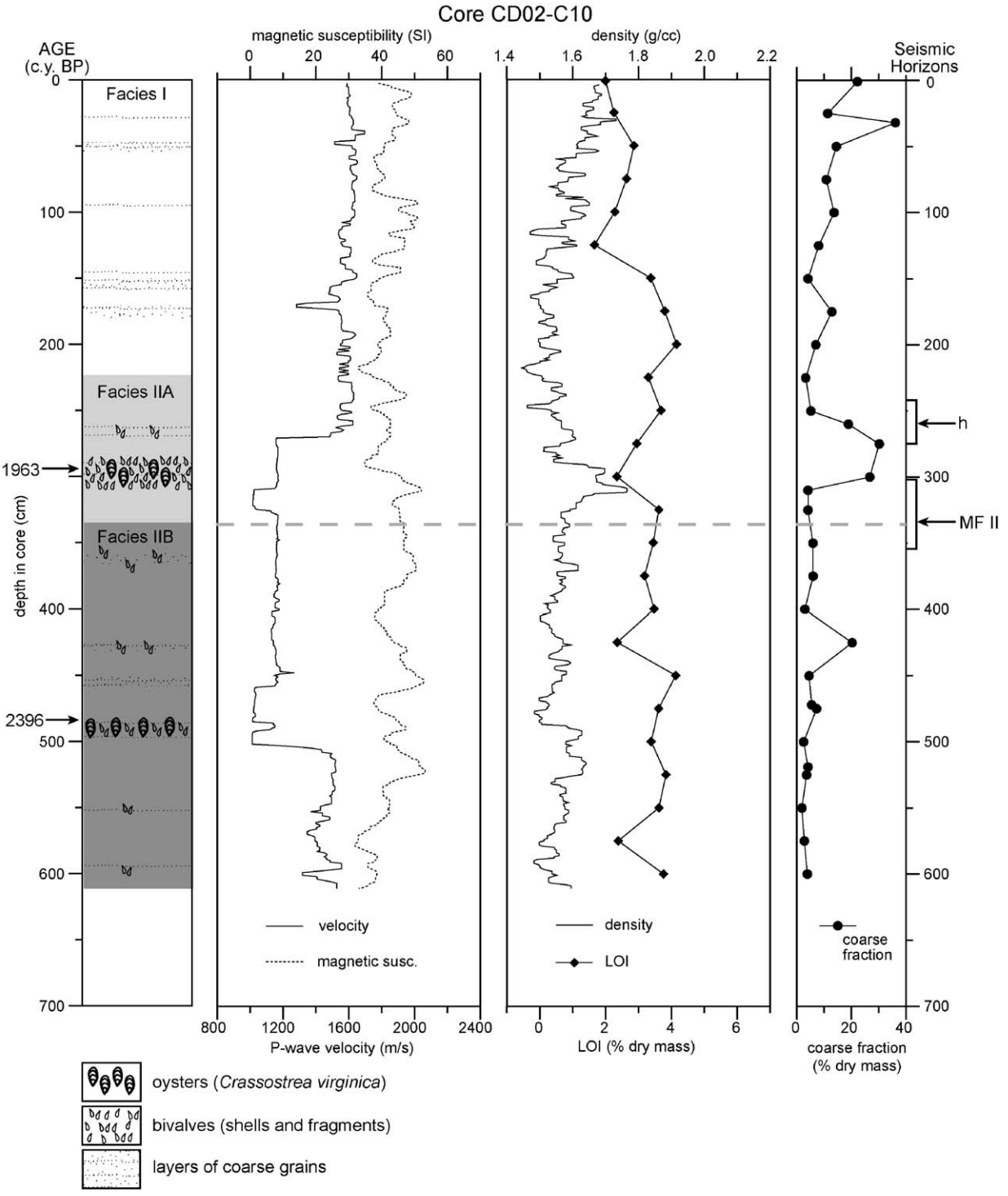

Fig. 7. Lithology, physical properties, and interpreted facies for core CD02-C10. Corrected radiocarbon ages are shown on the left. Prominent seismic horizons are indicated by arrows on the right (assuming a sediment velocity of 1500 m/s); bars show possible horizons depths for a range of sediment velocities, from 1400 to 1600 m/s. Horizon MF II, discussed in the text, is labeled on the right and indicated by a heavy dashed line.

Please cite this article as: A.L. Slagle et al., Late-stage estuary infilling controlled by limited accommodation space in the Hudson River, Marine Geology (2006), doi:10.1016/j.margeo.2006.07.009.

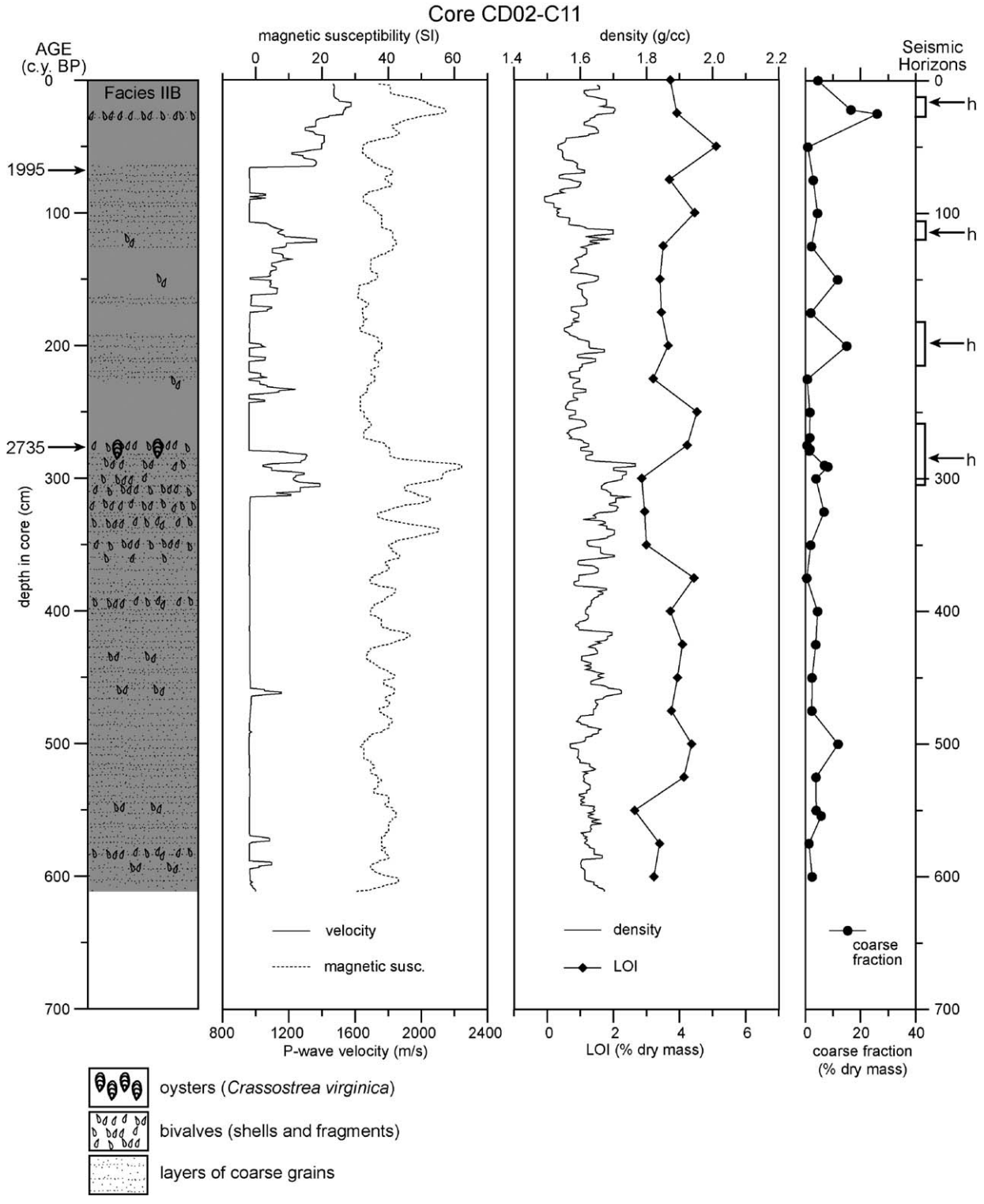

Fig. 8. Lithology, physical properties, and interpreted facies for core CD02-C11. Corrected radiocarbon ages are shown on the left. Prominent seismic horizons are indicated by arrows on the right (assuming a sediment velocity of 1500 m/s); bars show possible horizon depths for a range of sediment velocities, from 1400 to 1600 m/s.

Please cite this article as: A.L. Slagle et al., Late-stage estuary infilling controlled by limited accommodation space in the Hudson River, Marine Geology (2006), doi:10.1016/j.margeo.2006.07.009.

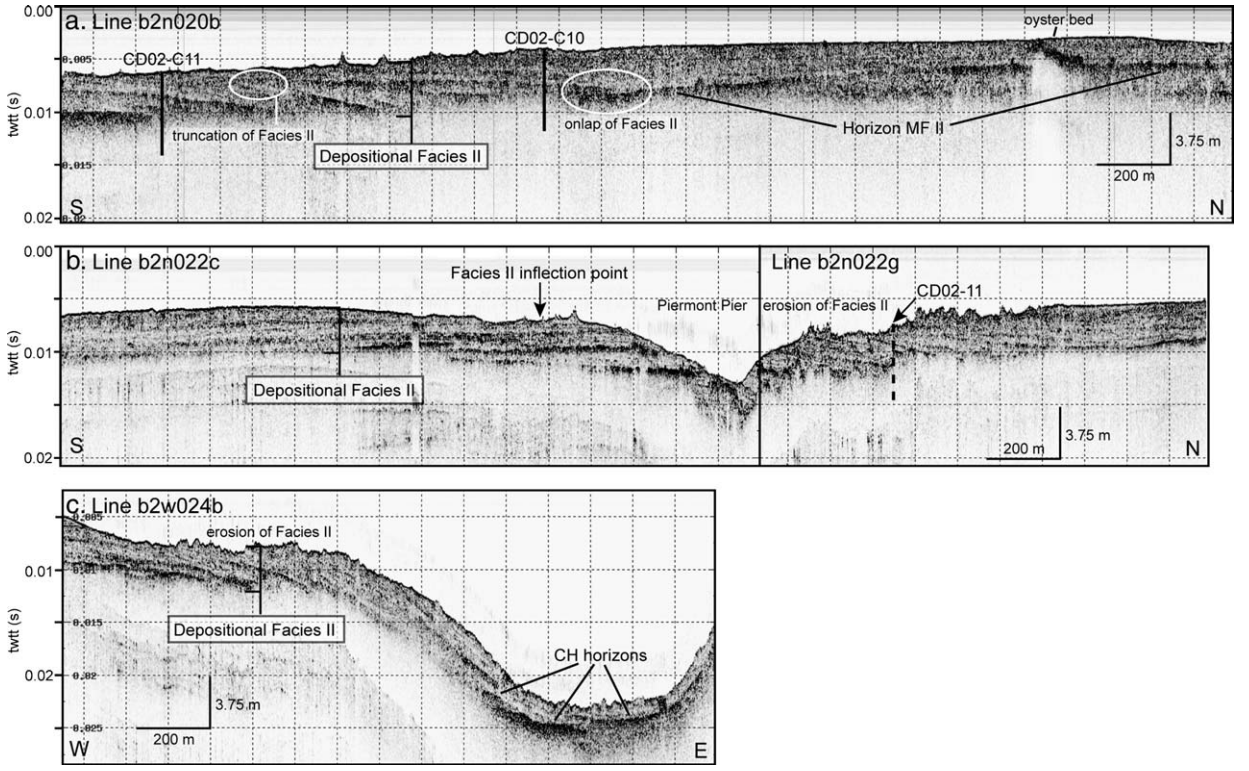

Fig. 9. Seismic profiles describing depositional Facies II. Seismic reflections of Facies II are dipping down toward the north and onlapping horizon MF II, described in the text. An oyster bed is imaged buried in the shallow subsurface (a). Facies II reflections dip northward to the north of the inflection point and southward, south of the inflection point labeled in (b). Fig. 9b is a composite of two north–south seismic lines, which are offset by ~10 m. Facies II reflections are truncated at the estuary floor (b and c), indicating that Facies II is no longer actively being deposited.

of the marginal flats west of the channel. It extends for ≥10 km in the northern part of the study area and is the dominant facies of the marginal flats, similar to the marginal flats sediments described farther south in the Hudson River Estuary (Carbotte et al., 2004; Klingbeil and Sommerfield, 2005) and in other estuaries such as the Chesapeake Bay (e.g. Baucom et al., 2001). Thinnest at its southern limit just south of the Tappan Zee Bridge, facies I is generally imaged to be ≥4 m thick. Except for the presence of horizons MF II and MF III, facies I is an acoustically transparent sediment package (Fig. 5b). Fossil oyster beds, documented by Carbotte et al. (2004) in this stretch of the estuary, appear as bright, acoustically impenetrable reflections in facies I (Figs. 5b and 6b–d). Oyster beds typically dip gently to the north, outcropping at their southern edges, but others are imaged in sub-bottom profiles buried by up to 3 m of sediment. Their lateral distribution suggests that these beds may have once stretched from bank to bank (Fig. 6; Carbotte et al., 2004).

Depositional facies I is sampled in a short gravity core (LWB2-14) and a longer vibra-core (~6 m, CD02-C10) collected for this study (Fig. 1, Table 1). Facies I sediments are dark gray to dark olive gray clay with rare bivalve fragments and rare layers of silty clay. Measured *P*-wave velocity is relatively high (~1600 m/s) and magnetic susceptibility is moderate, varying between 35 and 50 SI. Gamma density is relatively high in the shallowest facies I sediments (~1.7 g/cc) but decreases gradually toward the base of the unit (Fig. 7). Loss on ignition (LOI) values for facies I sediments are relatively low (<3%), indicating low organic content. From grain size measurements at 25-cm intervals, the average proportion of dry mass greater than 63 μm ("coarse fraction") ranges from 5% to 35%. Facies I is also sampled in vibra-core SD30 (Carbotte et al., 2004; Pekar et al., 2004). At this location, facies I sediments are characterized by similarly high *P*-wave velocity and somewhat lower magnetic susceptibility. Radiocarbon dates indicate low sedimentation rates of 1–2 mm/yr. LOI values from facies I in core SD30 (~3.5%), measured for this study, are slightly higher than values measured for this facies in our cores to the south.

Please cite this article as: A.L. Slagle et al., Late-stage estuary infilling controlled by limited accommodation space in the Hudson River, Marine Geology (2006), doi:10.1016/j.margeo.2006.07.009.

4.2.2. Facies II

Depositional facies II is comprised of a distinct series of dipping seismic reflections that occupy portions of the west marginal flats and west channel banks south of the Tappan Zee Bridge (Figs. 5a and 9a–c). This sediment package extends from the mouth of the freshwater Sparkill Creek as a lobe-shaped deposit, extending 7 km along-estuary and approximately 2 km across-estuary (Fig. 6b–d). In sub-bottom profiles, facies II is >4 m thick and thins toward the margins of its mapped extent. This seismically-defined sequence is characterized by bright, continuous reflections, dipping away from the western shore of the estuary toward the channel. There is an inflection point in facies II, north of which the reflections dip to the north and south of which, reflections dip to the south (Fig. 9b). The inflection point occurs at the same latitude as the mouth of the Sparkill Creek, a tributary that enters the estuary from the west through the Piermont Marsh (Fig. 6b–d).

At the northern extent of facies II, dipping reflections within the sequence onlap the prominent, southward-dipping marginal flats horizon, MF II (Figs. 5a and 9a). Horizon MF II divides facies II into two subunits (IIA and IIB), with the younger subunit IIA lying above horizon MF II. The mapping of deeper reflections within the dipping sequence (facies IIB) indicates a longer history of facies II deposition, although existing age control does not allow us to constrain the maximum age of the sequence. In addition to the onlapping relationship between facies II reflections and horizon MF II, dipping facies II reflections are imaged onlapping bright horizontal to sub-horizontal internal reflections at the southern extent of the study area. There is also evidence of truncation of dipping facies II reflections against other bright reflections internal to the sequence (Fig. 9a).

Sub-bottom data provide stratigraphic evidence that facies II deposition did not continue into the modern period of estuarine sedimentation. South of the Tappan Zee Bridge, the acoustically transparent sediments of facies I are imaged above the shallowest dipping horizon of the facies II package (Figs. 5a and 9a). In the southern half of the study area where facies I is not imaged above facies II, the modern riverbed has been eroded, evidenced by truncation of dipping facies II reflections at the river bottom (Figs. 5a and 9b–c).

The lithology of depositional facies II is revealed in two 6-m vibra-cores, CD02-C10 and CD02-C11 (Figs. 7 and 8). Sediments of facies II consist of black to dark gray silty clay with rare to common small (0.5–2.0 cm) bivalve shells and shell fragments. *P*-wave velocity is relatively high in the shallowest facies II sediments but the majority of facies II registers lower velocity values than facies I, which we attribute to gassy sediment or cracks in the cores. Magnetic susceptibility ranges between 30 and 65 SI and has less high frequency variability than facies I sediments. Gamma density in facies II is similar in range to facies I, but also shows less high frequency variability than in facies I sediments. LOI values for facies II (≥3%) are slightly higher than facies I sediments. Our grain size data indicate that the coarse fraction (>63 μ) in facies II sediments is low but variable, ranging from 1% to 35% of the total dry mass. Peaks in coarse fraction are associated with abundant quartz and often decreased organic material, based on microscopic examination of sediment sub-samples.

Facies IIA (the younger subunit) within core CD02-C10 has a ~15 cm thick layer of mixed shells and shell fragments, including oysters and small bivalves. From radiocarbon dating this material, we estimate that facies IIA was deposited between ~1700 and 2100 BP at a rate of 2–4 mm/yr. Facies IIB (the older subunit) includes millimeter to centimeter-scale layers of sand-sized grains, sometimes containing shells and shell fragments. Local highs in magnetic susceptibility and gamma density coincide with these shelly, coarse-grained layers (Fig. 8). These layers are also coincident with the depths of bright, dipping reflections in seismic profiles. From our data we cannot determine the depth extent of facies IIB, which extends beyond the reach of sediment cores, but one of the dipping reflections within this subunit has been dated with a maximum age of 2735 BP (Fig. 8).

5. Interpretation and discussion

5.1. Sparkill Creek Delta Deposit

We interpret depositional facies II as a subaqueous delta deposit sourced from the Sparkill Creek (Fig. 6b–d). In modern and ancient systems, deltas are recognized by internal structure, vertical and lateral geometry, and sedimentary characteristics (e.g. Boggs, 1995; Piggot, 1995). The internal geometry of facies II is consistent with a deltaic origin. Bright, dipping reflections in facies II are interpreted as clinoforms. Facies II reflections onlap the internal horizon MF II, as deltaic wedges prograde across the erosional surface (Fig. 9a–c). The inflection point in facies II, north of which reflections dip down to the north and south of which reflections dip down to the south, is at the same latitude as the mouth of the Sparkill Creek (Fig. 6b–d). In map view, facies II forms a lobe shape typical of deltaic deposits. From the point at which the modern Sparkill Creek enters the estuary, the deposit extends farther to the south than to the north, which may reflect the mixed influence of unidirectional

Please cite this article as: A.L. Slagle et al., Late-stage estuary infilling controlled by limited accommodation space in the Hudson River, Marine Geology (2006), doi:10.1016/j.margeo.2006.07.009.

downstream flow and bidirectional tidal flow during the period of active deposition. Sediment cores from the Piermont Marsh indicate that the course of the Sparkill Creek through the marsh has not changed appreciably in the past 1400 yr, suggesting a stable geographic relationship between the tributary mouth and the facies II sequence (Pederson et al., 2005).

Typically, delta deposits are more coarse-grained than the background sedimentation. Grain size data for cores in this study area suggest that facies II is not coarser than the background sedimentation on the nearby marginal flats. The fine-grained nature of this deposit could reflect the predominance of relatively soft material (siltstone and shale) of the Newark Basin within the watershed of the Sparkill Creek (Isachsen et al., 2000). The geographic location of the Sparkill Creek, in the mesohaline part of the estuary, may also play a role. Hypopycnal flow is expected in this setting, with fine sediment carried in suspension in the fresh water of the tributary before it reaches the more saline estuarine waters in the Tappan Zee–Piermont area, where it flocculates and settles from suspension. This type of flow in classic fluvial or lacustrine systems results in a delta of muddy composition (e.g. Boggs, 1995). Sedimentation rates for facies II (2–4 mm/yr) are higher than those estimated for the adjoining marginal flats (facies I; 1–2 mm/yr). These locally enhanced deposition rates are also consistent with delta deposition.

Fine-grained deposits are also identified at the mouths of several small tributaries to the Tappan Zee area, while only coarse-grained tributary deposits are found farther north in the estuary (Bell et al., 2000). Nitsche et al. (2006) presented side-scan sonar data showing delta-like deposits at the mouths of a number of northern tributaries to the Hudson River Estuary. These lobes or fan shaped features are characterized by high backscatter and are elongate along the shoreline. They are smaller than the Sparkill Creek Delta Deposit (facies II), typically extending 1–2 km along the estuary and <500 m away from the shoreline. Sediment sampling indicates that these delta-like accumulations are typically coarser-grained than surrounding bottom sediments, in contrast to the Sparkill Creek Delta Deposit and adjacent marginal flats. Most of these tributaries enter the estuary in the fresher reaches, north of the Hudson Highlands. Flows into the estuary in these areas are most likely homopycnal, with tributary and basin waters being of relatively equivalent densities. Under these conditions, coarse material settles out due to the change in flow regime as the tributary enters the estuary (e.g. Boggs, 1995), but without the density-enhanced flocculation and deposition of fine-grained material expected for hypopycnal flows. The morphology in the northern reaches is also different from the morphology near the Sparkill Creek. The northern stretch of the estuary is significantly narrower than the wide Tappan Zee bay and there are no broad marginal flats developed along the channel (e.g. Coch and Bokuniewicz, 1986; Bell et al., 2004), so hydrodynamic conditions may not be favorable for fine-grained deposition. These differences may explain the lack of large delta deposits comparable to the Sparkill Creek Delta Deposit, associated with the larger, northern tributaries.

The rapid accumulation and fine-grained nature of facies II could reflect an estuarine turbidity maximum deposit. Based on paleosalinity estimates and sedimentation rates, Pekar et al. (2004) postulated a paleo-estuarine turbidity maximum (ETM) in the Tappan Zee area of the Hudson River Estuary ~3400 BP, which migrated south of the Tappan Zee area prior to 2600 BP. Relatively rapid deposition of fine-grained estuarine sediments is expected at an ETM, where fine-grained suspended sediment undergoes coagulation due to the convergence of salt and fresh-water flows and the reduction in turbulence caused by the salinity-induced density gradient (Olsen et al., 1978; Nichols et al., 1991; Geyer, 1993; Jaeger and Nittrouer, 1995). However, we favor a deltaic interpretation for the facies II sequence based on our chronology, which reveals that facies II sedimentation began prior to 2700 BP, older than the estimated timing of the passage of a paleo-ETM. In addition to this age discrepancy, ETM-driven sedimentation cannot account for the unique dipping geometry of the facies II sequence north and south of the Sparkill Creek.

5.2. Variations in deposition through time

Sediment, stratigraphic, and radiocarbon data indicate that sediment deposition associated with the Sparkill Creek Delta Deposit has not been continuous over the past 3000 yr. Delta deposition (facies II) dominated the marginal flats east of the Sparkill Creek prior to 2700 BP. After more than 1000 yr of relatively rapid accumulation, delta deposition ceased ~1700 BP, followed by a period of slower deposition during which the acoustically transparent marginal flats sediments (facies I) were deposited above the delta sediments. Deposition of these marginal flats sediments most likely continued until the modern period, which is largely characterized by erosion and scour of the river bed (Fig. 6a). Our data show that dipping reflections from the Sparkill Creek Delta Deposit are truncated at the estuary floor over an area of ~3 km northeast and south of the Piermont Pier

Please cite this article as: A.L. Slagle et al., Late-stage estuary infilling controlled by limited accommodation space in the Hudson River, Marine Geology (2006), doi:10.1016/j.margeo.2006.07.009.

(Figs. 5a and 9b–c). Gamma spectroscopy results from this and previous studies show that ^{137}Cs is not detected in the majority of surface samples from the marginal flats in this area (Fig. 6a and Table 1; McHugh et al., 2004). The primary source of ^{137}Cs to the Hudson River region is global fallout from nuclear weapons tests and other nuclear activities, and it was not present in the environment prior to ~1950. The absence of ^{137}Cs indicates that the marginal flats were not accumulating new sediments over the last 50 yr. The one exception is a confined region of sediment accumulation directly northwest of the Piermont Pier (Fig. 6a; Nitsche et al., 2005). Although we cannot establish the precise timing of erosion and local deposition, changes in local hydrodynamic conditions accompanying construction of the Piermont Pier beginning in 1839 likely contributed to the modern sedimentary pattern.

Discontinuous sedimentation is also evident in the seismic horizons mapped through the Tappan Zee–Piermont area, which appear to represent discrete intervals of erosion or nondeposition over the past 3500 yr. They are mapped across the estuary, within the marginal flats, channel banks, and channel regimes. These surfaces are characterized by layers of shells and fragments and abrupt changes in physical properties in sediment cores (Figs. 4, 7, and 8), consistent with an erosional or nondepositional origin. The youngest interval of erosion or nondeposition (*Surface 1*) is recorded in the channel banks, represented by horizons CB I north and CB I central (Fig. 6b). Radiocarbon data place this surface at or before 1600 BP, as our dates provide maximum age constraints for seismic horizons. *Surface 2* is dated between 2100–2210 BP. This surface is represented by horizon MF II in the marginal flats and CB II in the channel bank sediments (Fig. 6c). Surface 2 interrupts delta deposition in the marginal flats and separates facies IIA and IIB. Dense wood layers with a similar age occur in core CD01-02, indicating that the erosion or nondepositional interval associated with Surface 2 may also be recorded in west channel bank sediments. The oldest surface identified, *Surface 3*, sits deep in the marginal flats and is represented by horizon MF III (Fig. 6d). A radiocarbon date from Carbotte et al. (2004) placed this surface at or prior to 3400 BP.

Fossil oyster beds lie above the erosion or nondeposition surfaces in the Tappan Zee–Piermont area and, in some places, appear to shoal up from them (Figs. 5b and 9a). Erosional surfaces may even have provided hard substrates suitable for oyster settlement and development (Carbotte et al., 2004). The oyster population thrived during two periods, ~500–2400 and ~5600–6100 BP, and grew during the slow deposition phase of facies I in the Tappan Zee–Piermont area (Carbotte et al., 2004). The oyster beds extend across the marginal flats in bands and may once have armored the estuary floor against erosion. However, oyster beds are cut by the modern channel, leaving remnants of eroded beds along the steep channel walls (Fig. 6b–d; Carbotte et al., 2004), indicating that they have been exhumed by erosional processes, such as those that likely formed the regional horizons we observe in the study area.

5.3. Limited accommodation space

The evidence we find near Sparkill Creek for periods of regional erosion or nondeposition with intervening periods of deposition may reflect sedimentation that is fundamentally controlled by limited accommodation space. During a phase of erosion, sediment is stripped from the estuary floor across a number of estuarine terrains, creating accommodation space and potentially leaving behind evidence such as our regional horizons. Klingbeil and Sommerfield (2005) observed similar reflections in post-colonial sediments farther south in the lower Hudson River Estuary and postulated that they represented the effects of modern events that enhance bottom erosion, such as storm surges or river floods. The modern sedimentary environment in the Tappan Zee–Piermont area (Fig. 6a), including that of the channel, channel banks, and marginal flats, is currently dominated by erosion or scour and nondeposition. Similar bottom processes are evident elsewhere in the modern Hudson River Estuary (Nitsche et al., 2004; McHugh et al., 2004; Klingbeil and Sommerfield, 2005), implying that discrete storm events are not required to create regionally extensive eroded surfaces. Seismic horizons may even represent an amalgamation of multiple periods of active erosion or sedimentary bypass.

We observe that a phase of relatively rapid deposition (2–4 mm/yr) overlying regional horizons follows the creation of accommodation space. In the Sparkill Creek Delta Deposit, the infilling period was restricted to approximately 1000 yr. We propose that deposition was chiefly limited by accommodation space, although additional factors such as temporal variations in sediment supply, tides, and estuary morphology may also have played substantial roles. This infilling process has an analogue in modern estuaries, where elevated sedimentation rates have been observed following removal of material by dredging activities (Meade, 1969; Bokuniewicz and Coch, 1986; Nichols and Howard-Strobel, 1991; Van der Wal et al., 2002). In the Hudson River Estuary, where dredging has taken place for more than 100 yr between the Battery and Troy, NY, there is evidence of a four-fold increase in local sedimentation

Please cite this article as: A.L. Slagle et al., Late-stage estuary infilling controlled by limited accommodation space in the Hudson River, Marine Geology (2006), doi:10.1016/j.margeo.2006.07.009.

rate following dredging of Haverstraw Bay and along the Manhattan stretch of the estuary (Ellsworth, 1986; Olsen et al., 1993; Abood and Metzger, 1996; Fountain, 2003).

Outside the areas of anthropogenic sediment removal, studies of long-term sediment accumulation support the notion that many parts of the Hudson River Estuary are now effectively filled to a state of morphological equilibrium. Olsen et al. (1978) estimated a long-term sedimentation rate of ~1.0 mm/yr, upstream of the inner harbor area of New York, which has kept pace with combined effects of sea-level rise and post-glacial isostatic rebound for the area (Peltier, 1999). McHugh et al. (2004) cited radiocarbon dates of shells and wood between 1000 and 3000 BP in shallow sediments and the presence of coal and other signs of coal burning scattered on the modern estuary floor as evidence of the absence of significant accumulation during the latest Holocene.

Alternating phases of erosion and deposition may be the mechanism by which the Hudson River Estuary maintains this morphological equilibrium through time. McHugh et al. (2004) concluded that Newburgh Bay, ~40 km north of the Tappan Zee area, reached a state of equilibrium at ~3000 BP, based on evidence of increased downstream bypass of suspended sediment in the sedimentary record. South of our study area, Klingbeil and Sommerfield (2005) interpreted shallow shoals along Manhattan to be accumulating with a long-term accretion rate that keeps up with sea-level rise. They also presented evidence of internal erosion surfaces, which were attributed to intermittent sediment removal by storms and river flooding events. Studies of accumulation rates in the Hudson River Estuary revealed a discrepancy between long-term (millennial) rates of 1–2 mm/yr and short-term (seasonal) rates of ~10 cm/yr (Geyer et al., 2001; Woodruff et al., 2001). This supports the notion that a state of equilibrium may be reached by balancing erosion events that remove sediment or nondeposition during periods of limited accommodation space with periods of accumulation when space is available.

5.4. Holocene sea-level and climate change

Correlations between sea-level change and coastal morphology are documented in many coastal regions (e.g. Stanley and Warne, 1994; Tanabe et al., 2003; Hori et al., 2004). Sea-level curves for the Holocene document a varied history that, in many locations, includes dramatic fluctuations in the rate of sea-level rise (e.g. Peltier, 1999). We postulate that the history of punctuated sedimentation in the Hudson River Estuary could reflect sea-level fluctuations. Records from along the U.S. Atlantic coast indicate a period of changing sea-level between 4000 and 1500 BP, contemporaneous with the period in which Surfaces 1, 2, and 3 were formed in the Tappan Zee–Piermont area of the Hudson River Estuary (Fig. 10). Although there is little detailed sea-level data for the Hudson River Valley, the model of Peltier (1998) shows a clear decline in the rate of sea-level rise for New York, NY at ~3100 BP. Radiocarbon dating of basal peats in the tidal marshes of Virginia, Delaware, and Maine indicates a deceleration in the rate of sea-level rise at ~4000 BP (Van de Plassche, 1990; Fletcher et al., 1993b; Kelley et al., 1995; Gehrels, 1999; Nikitina et al., 2000). Decreasing rates of sea-level rise are documented between 3200 and 2000 BP in New York, Connecticut, and New Jersey (Stuiver and Daddario, 1963; Rampino, 1979; Van de Plassche et al., 1989, 2002), during the older phase of delta deposition (facies IIB) in our study. Two prominent wood layers within channel bank sediments of the Tappan Zee–Piermont region close in age to regional horizons MF II and CB II may be linked to the formation of Surface 2 (Fig. 10; Table 2). A rise in the rate of sea-level is documented at 1800 BP in the tidal marshes and wetlands of Connecticut, New Jersey, and Delaware (Meyerson, 1972; Van de Plassche, 1991; Fletcher et al., 1993a,b; John and Pizzuto, 1995). On a broader scale, global sea-level and paleoclimate proxies reveal several minima in Red Sea sea-level (Siddall et al., 2003) and in Sargasso Sea carbonate data, indicating increased terrigenous input and cooler temperatures (Keigwin, 1996) during the significant interval between 4000 and 1500 BP (Fig. 11). Lake sediments from Vermont (Noren et al., 2002) and Florida (Liu and Fearn, 2000) reveal changes in large-scale atmospheric circulation patterns in the northeastern U.S. during the critical interval.

A sedimentary system with limited accommodation space would be expected to be particularly sensitive to relatively small sea-level changes. During a transgression (a steady-state increase of sea-level or increase in the rate of sea-level rise), accommodation space would be created, leading to sediment accumulation. Vertical space created by a transgression in the lower Hudson River Estuary could account for delta deposition at the mouth of the Sparkill Creek, with delta deposition continuing to accumulate as long as accommodation space and sediment supply were adequate. Hypopycnal flow would be amplified by the contrast between fresh tributary waters and rising marine waters, favoring the deposition of a muddy delta such as the Sparkill Creek

Please cite this article as: A.L. Slagle et al., Late-stage estuary infilling controlled by limited accommodation space in the Hudson River, Marine Geology (2006), doi:10.1016/j.margeo.2006.07.009.

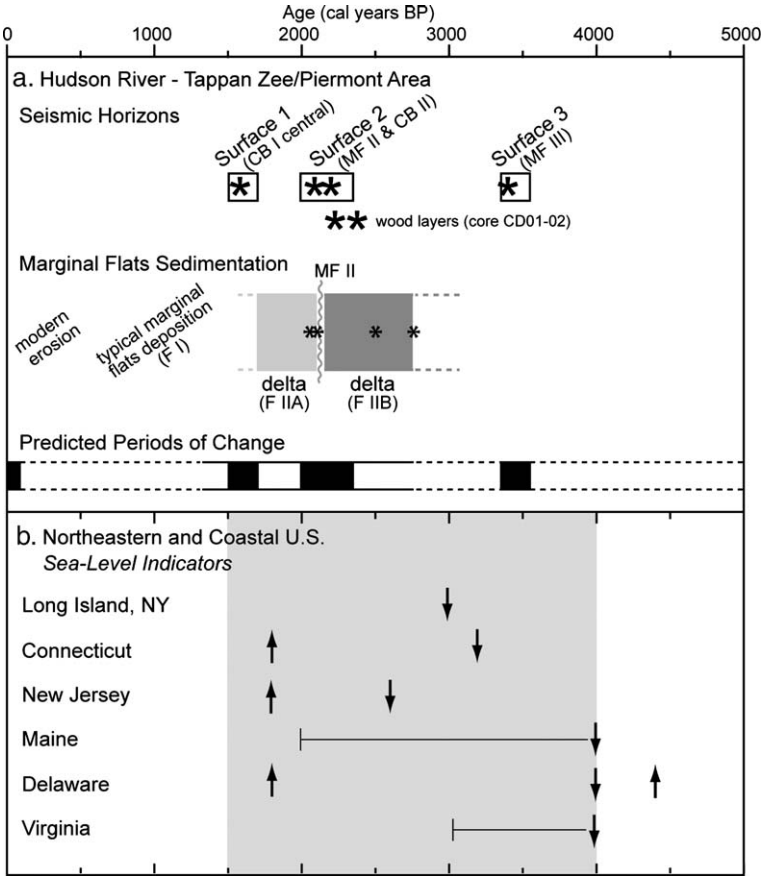

Fig. 10. Comparison of Tappan Zee–Piermont chronology for seismic horizons and sedimentary patterns with sea-level changes from the northeastern and coastal United States. (a) Ages for regional horizons are indicated by black asterisks and erosion surfaces are shown as boxes. Two prominent wood layers, indicated by offset asterisks, in core CD01-02 in the channel banks (see Fig. 1; Table 2) may be contemporaneous with erosional Surface 2. The overview of marginal flats sedimentation shows the Sparkill Creek Delta Deposit (Facies II) followed by typical marginal flats deposition (Facies I), which ultimately gives way to erosion in the modern setting. Small black asterisks indicate radiocarbon-dated samples within the delta deposit. The alternating bar shows our prediction for sea-level rise history in the Hudson, assuming nondeposition or phases of erosion coincide with periods of rapid changes in sea-level (black bars); phases of sediment deposition would coincide with relatively constant sea-level rise conditions (white bars). Dashed lines indicate periods of uncertainty. (b) Changes in sea-level during the mid-late Holocene along the western Atlantic coast, based on records from tidal marshes. Arrows pointing down indicate dropping rate of sea-level rise; arrows pointing up indicate increasing rate of sea-level rise. Data for Long Island are from Rampino (1979); Connecticut from Van de Plassche et al. (1989), Van de Plassche (1991), Nydick et al. (1995), and Van de Plassche et al. (2002); New Jersey from Stuiver and Daddario (1963) and Meyerson (1972); Maine from Kelley et al. (1995) and Gehrels (1999); Delaware from Fletcher et al. (1993a,b), John and Pizzuto (1995), and Nikitina et al. (2000); and Virginia from Van de Plassche (1990). The gray shaded area indicates the period between 4000 and 1500 BP in which erosion or nondeposition occurred in the Tappan Zee–Piermont area of the Hudson River Estuary.

Delta Deposit. During a regression, removal of sediment from the estuary floor would be expected due to the fall in base level. A drop in rate of sea-level rise may be sufficient to transform an area of active deposition into one of sedimentary bypass, creating a nondepositional surface rather than one of active erosion. We speculate that seismic Surfaces 1, 2, and 3 could reflect periods of regression or decreased rates of sea-level rise. The Tappan Zee–Piermont area would be fresher than today due to the receding of marine waters during a regression. Hypopycnal conditions at the mouths of freshwater tributaries, such as the Sparkill Creek, would be dampened by the decrease in density contrast between tributary and estuary waters. This could also contribute to a reduction in fine-grained sediment accumulation in this area.

5.5. Hudson River Estuary compared to a classic coastal plain estuary

The post-glacial geologic history of the Hudson River Estuary as a fjord filled by proglacial lake sediments

Please cite this article as: A.L. Slagle et al., Late-stage estuary infilling controlled by limited accommodation space in the Hudson River, Marine Geology (2006), doi:10.1016/j.margeo.2006.07.009.

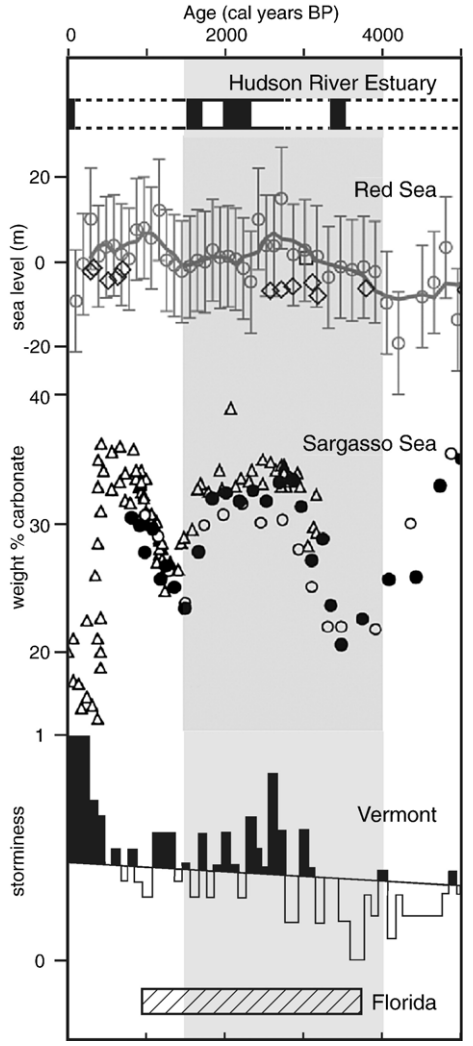

Fig. 11. Sea-level and climate proxy data for the mid-late Holocene. Based on observations of seismic surfaces and depositional facies in the Hudson, we predict an alternating pattern of rapid changes in sea-level (black bars) and relatively constant sea-level conditions (white bars); see Fig. 10. Sea-level reconstruction based on $\delta^{18}O$ from the Red Sea (from Siddall et al., 2003; gray curve and gray symbols are Red Sea data, black symbols are values from coral studies). Weight % carbonate record from the Sargasso Sea (from Keigwin, 1996; symbols correspond with data from three different cores as described in original source). Storminess histogram showing terrigenous sedimentation events from 13 Vermont lakes (from Noren et al., 2002; values above linear regression line are shaded, as described in original source). Data from a northwestern Florida lake reveal a period of increased frequency of catastrophic hurricanes between ~950 and 3700 BP (from Liu and Fearn, 2000; rectangle indicates "hyperactive" period, based on sand layers in a coastal lake core). The interval highlighted in gray, between 4000 and 1500 BP, indicates the time period during which three prominent regional horizons were created in the Tappan Zee–Piermont area of the Hudson River Estuary.

distinguishes it from classic drowned river valleys, such as the Chesapeake Bay. During the retreat of the Laurentide ice sheet, meltwater was impounded between terminal moraines and much of the Hudson Valley was covered by glacial lakes (Uchupi et al., 2001; Donnelly et al., 2005). Lacustrine sediments accumulated on top of glacial till and bedrock, filling much of the valley of the Hudson River. Following the breach of the terminal moraines, meltwater from the lakes drained to the sea, eroding a new fluvial channel into the lacustrine sediments. The remaining space has been almost completely filled by the relatively thin package of fluvial and estuarine sediments that has been accumulating since the time brackish water invaded the Hudson River (Worzel and Drake, 1959; Newman et al., 1969; Weiss, 1974). Stratigraphic profiles, developed from seismic observations and bridge borings, indicate that >80% of the sedimentary infill is lacustrine sediments, while <20% is estuarine sediments (Worzel and Drake, 1959; Newman et al., 1969).

The Chesapeake Bay Estuary is an example of a classic coastal plain estuary with much greater accommodation space. The paleochannel established during the last glacial lowstand is directly overlain by estuarine sediments and has been only partially filled during the Holocene transgression (Colman et al., 1990, 1992; Cronin et al., 2000). In the absence of sea-level changes, the present bay would require ~10,000 yr to fill with sediment (Colman et al., 1992). The Chesapeake Bay has evolved with a significant amount of storage space for estuarine sediment and is currently dominated by deposition enhanced by anthropogenic activities (Brush, 1984; Cooper and Brush, 1991; Cronin, 2000; Cronin et al., 2000; Colman et al., 2002; Willard et al., 2003). In contrast, the sedimentary patterns of deposition and erosion in the modern Hudson River Estuary, with its particular post-glacial history, are consistent with a system fundamentally limited by the availability of accommodation space.

6. Conclusions

For the Tappan Zee–Piermont area of the Hudson River Estuary, the sedimentary record reveals a late Holocene history in which intervals of deposition alternate with episodes of erosion. The Sparkill Creek Delta (facies II) represents a period of relatively rapid deposition on the marginal flats between ~2700 and 1700 BP, followed by a period of slower accumulation of facies I. However, the modern estuary floor in this area is dominated by erosion and scour rather than deposition. Between periods of deposition, a series of sub-bottom horizons indicate hiatuses in deposition, which we

Please cite this article as: A.L. Slagle et al., Late-stage estuary infilling controlled by limited accommodation space in the Hudson River, Marine Geology (2006), doi:10.1016/j.margeo.2006.07.009.

interpret to be erosional or nondepositional intervals. We find evidence of at least three phases of erosion between 4000 and 1500 BP, an interval that corresponds with a period of fluctuating sea-level and climate change in the North Atlantic Ocean and in Europe.

The Hudson River Estuary evolved from a glacially carved fjord that was partially filled with lacustrine and possibly fluvial sediments, leaving limited space for additional accumulation of estuarine sediment. In a sedimentary environment that is fundamentally space-limited, even small fluctuations in sea-level may be expressed as significant depositional intervals during an increase in the rate of sea-level rise or major erosion intervals during a fall in the rate of sea-level rise. While in many coastal environments, sedimentary patterns are controlled by wave or tidal energy and sediment supply, sedimentary patterns in the Hudson River Estuary may be primarily controlled by its evolving morphology and changing sea-level. The identification of space-limited sedimentary patterns may be applicable in other glacially-influenced estuaries and may distinguish them from the classic model of coastal plain estuaries.

Acknowledgements

We would like to thank the many people who were involved in the collection and processing of the data, including R. Arko and J. Ardai. Special thanks go to N. Anest and R. Lotti for their help with core physical properties and photography, and to D. Peteet, S. Hemming, and M. Mendelson for their assistance with sediment analysis. We thank J. Lipscomb of the Riverkeeper, the captain and crew of the *R/V Walford* of the New Jersey Marine Consortium, and Ocean Surveys, Inc. and crew for their excellent support during survey and sampling operations. We also thank T. Guilderson of Lawrence Livermore National Labs for radiocarbon analysis. We thank C. McHugh, S. Nichol, and an anonymous reviewer for their comments, which improved the paper. The New York State Department of Environmental Conservation provided funding for the primary data acquisition from the Environmental Protection Fund through the Hudson River Estuary Program. This research was also funded in part by the Estuarine Reserves Division, Office of Ocean and Coastal Resource Management, National Ocean Service, National Oceanic and Atmospheric Administration (award NA16OR2405) and the Hudson River Foundation (grant 003A/00A to SMC and REB). Lamont-Doherty Earth Observatory contribution no. 6929.

References

Abood, K.A., Metzger, S.G., 1996. Comparing impacts to shallow-water habitats through time and space. Estuaries 19 (2A), 220–228.

Allen, G.P., Posamentier, H.W., 1994. Transgressive facies and sequence architecture in mixed tide- and wave-dominated incised valleys: example from the Gironde Estuary, France. In: Dalrymple, R.W., Boyd, R., Zaitlin, B.A. (Eds.), Incised-valley Systems: Origin and Sedimentary Sequences. SEPM (Society for Sedimentary Geology) Special Publication, vol. 51, pp. 225–240.

Baucom, P.C., Bratton, J.F., Colman, S.M., Moore, J.M., King, J., Heil, C., Seal II, R.R., 2001. Selected Data for Sediment Cores Collected in Chesapeake Bay in 1996 and 1998. 01-194, Department of Interior/ U.S. Geological Survey.

Bell, R.E., Flood, R., Carbotte, S.M., Ryan, W.B.F., McHugh, C.M.G., Cormier, M.-H., Versteeg, R., Chayes, D., Bokuniewicz, H., Ferrini, V., Thissen, J., 2000. Hudson River Estuary Program Benthic Mapping Project: Phase I Final Report to New York State Department of Environmental Conservation, Lamont-Doherty Earth Observatory, SUNY Stony Brook, Queens College.

Bell, R.E., Flood, R., Carbotte, S.M., Ryan, W.B.F., Nitsche, F.O., Chilrud, S., Arko, R., Ferrini, V., Slagle, A., Bertinato, C., Turrin, M., 2004. Hudson River Estuary Program Benthic Mapping Project, Phase III—Report I to New York State Department of Environmental Conservation, Lamont-Doherty Earth Observatory, SUNY Stony Brook.

Bell, R.E., Flood, R.D., Carbotte, S.M., Ryan, W.B.F., McHugh, C.M.G., Cormier, M., Versteeg, R., Bokuniewicz, H.J., Ferrini, V., Thissen, J., Ladd, J.W., Blair, E.A., 2006. Benthic habitat mapping in the Hudson River Estuary. In: Levinton, J.S., Waldman, J.R. (Eds.), The Hudson River Estuary. Cambridge University Press, pp. 51–64.

Boggs, S., 1995. Principles of Sedimentology and Stratigraphy. Prentice-Hall, Inc., Upper Saddle River, New Jersey. 774 pp.

Bokuniewicz, H.J., Coch, N.K., 1986. Some management implications of sedimentation in the Hudson-Raritan estuarine system. Northeast. Geol. 8 (3), 165–170.

Brush, G.S., 1984. Patterns of recent sediment accumulation in Chesapeake Bay (Virginia Maryland, USA) tributaries. Chem. Geol. 44 (1–3), 227–242.

Carbotte, S.M., Bell, R.E., Ryan, W.B.F., McHugh, C.M.G., Slagle, A., Nitsche, F.O., Rubenstone, J., 2004. Environmental change and oyster colonization within the Hudson River Estuary linked to Holocene climate. Geo Mar. Lett. 24 (4), 212–224.

Coch, N.K., Bokuniewicz, H., 1986. Oceanographic and geologic framework of the Hudson system. Northeast. Geol. 8 (3), 96–108.

Colman, S.M., Halka, J.P., Hobbs, C.H., Mixon, R.B., Foster, D.S., 1990. Ancient channels of the Susquehanna River beneath Chesapeake Bay and the Delmarva peninsula. Geol. Soc. Amer. Bull. 102 (9), 1268–1279.

Colman, S.M., Halka, J.P., Hobbs III, C.H., 1992. Patterns and rates of sedimentation in Chesapeake Bay during the Holocene rise in sea level. In: Fletcher, C., Wehmiller, J.F. (Eds.), Patterns and Rates of Sedimentation in Chesapeake Bay during the Holocene Rise in Sea Level. Society of Economic Paleontologists and Mineralogists Special Publication, vol. 48, pp. 101–111.

Colman, S.M., Baucom, P.C., Bratton, J.F., Cronin, T.M., McGeehin, J.P., Willard, D., Zimmerman, A.R., Vogt, P.R., 2002. Radiocarbon dating, chronologic framework, and changes in accumulation rates of Holocene estuarine sediments from Chesapeake Bay. Quat. Res. 57, 58–70.

Please cite this article as: A.L. Slagle et al., Late-stage estuary infilling controlled by limited accommodation space in the Hudson River, Marine Geology (2006), doi:10.1016/j.margeo.2006.07.009.

Cooper, S.R., Brush, G.S., 1991. Long-term history of Chesapeake Bay anoxia. Science 254 (5034), 992–996.

Cronin, T.M., 2000. Initial Report on IMAGES V Cruise of the Marion-Dufresne to the Chesapeake Bay June 20-22, 1999. 00-306, U.S. Department of Interior/ U.S. Geological Survey.

Cronin, T.M., Willard, D., Karlsen, A., Ishman, S., Verardo, S., McGeehin, J.P., Kerhin, R., Holmes, C., Colman, S.M., Zimmerman, A.R., 2000. Climatic variability in the eastern United States over the past millennium from Chesapeake Bay sediments. Geology 28 (1), 3–6.

Dabrio, C.J., Zazo, C., Goy, J.L., Sierro, F.J., Borja, F., Lario, J., Gonzalez, J.A., Flores, J.A., 2000. Depositional history of estuarine infill during the last postglacial transgression (Gulf of Cadiz, Southern Spain). Mar. Geol. 162 (2-4), 381–404.

Dalrymple, R.W., Zaitlin, B.A., Boyd, R., 1992. Estuarine facies models — conceptual basis and stratigraphic implications. J. Sediment. Petrol. 62 (6), 1130–1146.

Dean, W.E., 1974. Determination of carbonate and organic matter in calcareous sediments and sedimentary rocks by loss on ignition: comparison with other methods. J. Sediment. Petrol. 44 (1), 242–248.

Donnelly, J.P., Driscoll, N.W., Uchupi, E., Keigwin, L.D., Schwab, W.C., Thieler, E.R., Swift, S.A., 2005. Catastrophic meltwater discharge down the Hudson Valley: a potential trigger for the Intra-Allerod cold period. Geology 33 (2), 89–92.

Ellsworth, J.M., 1986. Sources and sinks for fine-grained sediment in the lower Hudson River. Northeast. Geol. 8 (3), 141–155.

Feng, H., Cochran, J.K., Hirschberg, D.J., Wilson, R.E., 1998. Small-scale spatial variations of natural radionuclide and trace metal distributions in sediments from the Hudson River Estuary. Estuaries 21 (2), 263–280.

Fletcher, C.H., Knebel, H.J., Kraft, J.C., 1992. Holocene depocenter migration and sediment accumulation in Delaware Bay — a submerging marginal marine sedimentary basin. Mar. Geol. 103 (1–3), 165–183.

Fletcher, C.H., Pizzuto, J.E., John, S., Vanpelt, J.E., 1993a. Sea-level rise acceleration and the drowning of the Delaware Bay coast at 1.8 Ka. Geology 21 (2), 121–124.

Fletcher, C.H., Vanpelt, J.E., Brush, G.S., Sherman, J., 1993b. Tidal wetland record of Holocene sea-level movements and climate history. Palaeogeogr. Palaeoclimatol. Palaeoecol. 102 (3–4), 177–213.

Fountain, K., 2003. The Concept of an Equilibrium Profile and the Effect of Dredging on Sedimentation in Two Reaches of the Hudson River Estuary. M.A. Thesis, Columbia University, New York, 20 pp.

Gehrels, W.R., 1999. Middle and Late Holocene sea-level changes in eastern Maine reconstructed from foraminiferal saltmarsh stratigraphy and AMS ^{14}C dates on basal peat. Quat. Res. 52 (3), 350–359.

Geyer, W.R., 1993. The importance of suppression of turbulence by stratification on the estuarine turbidity maximum. Estuaries 16 (1), 113–125.

Geyer, W.R., Signell, R.P., Kineke, G.C., 1998. Lateral trapping of sediment in a partially mixed estuary. In: Dronkers, Scheffers (Eds.), Physics of Estuaries and Coastal Seas. Balkema, Rotterdam, pp. 115–124.

Geyer, W.R., Woodruff, J.D., Traykovski, P., 2001. Sediment transport and trapping in the Hudson River Estuary. Estuaries 24 (5), 670–679.

Hansen, L., 2004. Deltaic infill of a deglaciated Arctic Fjord, East Greenland: sedimentary facies and sequence stratigraphy. J. Sediment. Res. 74 (3), 422–437.

Heap, A.D., Nichol, S.L., 1997. The influence of limited accommodation space on the stratigraphy of an incised-valley succession: Weiti River estuary, New Zealand. Mar. Geol. 144 (1–3), 229–252.

Hori, K., Tanabe, S., Saito, Y., Haruyama, S., Nguyen, V., Kitamura, A., 2004. Delta initiation and Holocene sea-level change: example from the Song Hong (Red River) delta, Vietnam. Sediment. Geol. 164 (3–4), 237–249.

Isachsen, Y.W., Landing, E., Auber, J.M., Rickard, L.V., Rogers, W.B., 2000. Geology of New York: A Simplified Account. New York State Museum Educational Leaflets, vol. 28. The New York State Geological Survey, New York State Museum, Albany, New York, USA. 294 pp.

Jaeger, J.M., Nittrouer, C.A., 1995. Tidal controls on the formation of fine-scale sedimentary strata near the Amazon river mouth. Mar. Geol. 125, 259–281.

Jervey, M.T., 1988. Quantitative geological modeling of siliciclastic tock sequences and their seismic expression. In: Wilgus, C.K., et al. (Ed.), Sea Level Changes: An Integrated Approach. Society of Economic Paleontologists and Mineralogists, Special Publication, vol. 42. SEPM, Tulsa, pp. 47–69.

John, S.J., Pizzuto, J.E., 1995. Accelerated sea-level rise 2,000 years BP in the Delaware Bay — stratigraphic evidence from the Leipsic River Valley, Delaware, USA. J. Coast. Res. 11 (3), 573–582.

Keigwin, L.D., 1996. The Little Ice Age and Medieval Warm period in the Sargasso Sea. Science 274 (5292), 1504–1508.

Kelley, J.T., Gehrels, W.R., Belknap, D.F., 1995. Late Holocene relative sea-level rise and the geological development of tidal marshes at Wells, Maine, USA. J. Coast. Res. 11 (1), 136–153.

Klingbeil, A.D., Sommerfield, C.K., 2005. Latest Holocene evolution and human disturbance of a channel segment in the Hudson River Estuary. Mar. Geol. 218 (1–4), 135–153.

Liu, K.B., Fearn, M.L., 2000. Reconstruction of prehistoric landfall frequencies of catastrophic hurricanes in northwestern Florida from lake sediment records. Quat. Res. 54 (2), 238–245.

McHugh, C.M.G., Pekar, S.F., Christie-Blick, N., Ryan, W.B.F., Carbotte, S., Bell, R., 2004. Spatial variations in a condensed interval between estuarine and open-marine settings: Holocene Hudson River Estuary and adjacent continental shelf. Geology 32 (2), 169–172.

Meade, R.H., 1969. Landward transport of bottom sediments in estuaries of the Atlantic coastal plain. J. Sediment. Petrol. 39 (1), 222–234.

Menon, M., Gibbs, R., Phillips, A., 1998. Accumulation of muds and metals in the Hudson River Estuary turbidity maximum. Environ. Geol. 34 (2–3), 214–222.

Meyerson, A.L., 1972. Pollen and paleosalinity analyses from a Holocene tidal marsh sequence, Cape May County, New Jersey. Mar. Geol. 12 (5), 335–357.

Newman, W.S., Thurber, D.L., Zeiss, H.S., Rokach, A., Musich, L., 1969. Late quaternary geology of the Hudson River Estuary: a preliminary report. Trans. N. Y. Acad. Sci. 31 (5), 548–569.

Nichols, M.M., Howard-Strobel, M.M., 1991. Evolution of an urban estuarine harbor — Norfolk, Virginia. J. Coast. Res. 7 (3), 745–757.

Nichols, M.M., Johnson, G.H., Peebles, P.C., 1991. Modern sediments and facies model for a microtidal coastal plain estuary, the James Estuary, Virginia. J. Sediment. Petrol. 61 (6), 883–899.

Nikitina, D.L., Pizzuto, J.E., Schwimmer, R.A., Ramsey, K.W., 2000. An updated Holocene sea-level curve for the Delaware coast. Mar. Geol. 171 (1–4), 7–20.

Nitsche, F.O., Bell, R.E., Carbotte, S.M., Ryan, W.B.F., Flood, R., 2004. Process-related classification of acoustic data from the Hudson River Estuary. Mar. Geol. 209 (1–4), 131–145.

Nitsche, F.O., Bell, R., Carbotte, S.M., Ryan, W.B.F., Slagle, A., Chillrud, S., Kenna, T., Flood, R., Ferrini, V., Cerrato, R.,

Please cite this article as: A.L. Slagle et al., Late-stage estuary infilling controlled by limited accommodation space in the Hudson River, Marine Geology (2006), doi:10.1016/j.margeo.2006.07.009.

McHugh, C., Strayer, D., 2005. Integrative acoustic mapping reveals Hudson River sediment processes and habitats. EOS, Trans. Am. Geophys. Union 86 (24), 225–229.

Nitsche, F.O., Ryan, W.B.F., Carbotte, S.M., Bell, R.E., Slagle, A., Bertinado, C., Flood, R., Kenna, T., McHugh, C., 2006. Regional Patterns and Local Variations of Sediment Distribution in the Hudson River Estuary. Estuarine, Coastal, and Shelf Sciences, in press. doi:10.1016/j.ecss.2006.07.021.

Noren, A.J., Bierman, P.R., Steig, E.J., Lini, A., Southon, J., 2002. Millennial-scale storminess variability in the northeastern United States during the Holocene epoch. Nature 419 (6909), 821–824.

Nydick, K.R., Bidwell, A.B., Thomas, E., Varekamp, J.C., 1995. A sea-level rise curve from Guilford, Connecticut, USA. Mar. Geol. 124 (1–4), 137–159.

Olsen, C.R., Simpson, H.J., Bopp, R.F., WIlliams, S.C., Peng, T.H., Deck, B.L., 1978. A geochemical analysis of the sediments and sedimentation in the Hudson Estuary. J. Sediment. Petrol. 48 (2), 401–418.

Olsen, C.R., Larsen, I.L., Mulholland, P.J., Vondamm, K.L., Grebmeier, J.M., Schaffner, L.C., Diaz, R.J., Nichols, M.M., 1993. The concept of an equilibrium surface—applied to particle sources and contaminant distributions in estuarine sediments. Estuaries 16 (3B), 683–696.

Pederson, D.C., Peteet, D.M., Kurdyla, D., Guilderson, T., 2005. Medieval Warming, Little Ice Age, and European impact on the environment during the last millennium in the lower Hudson Valley, New York, USA. Quat. Res. 63 (3), 238–249.

Pekar, S.F., McHugh, C.M.G., Christie-Blick, N., Jones, M., Carbotte, S.M., Bell, R.E., Lynch-Stieglitz, J., 2004. Estuarine processes and their stratigraphic record: paleosalinity and sedimentation changes in the Hudson Estuary (North America). Mar. Geol. 209 (1–4), 113–129.

Peltier, W.R., 1998. Postglacial variations in the level of the sea: implications for climate dynamics and solid-earth geophysics. Rev. Geophys. 36 (4), 603–689.

Peltier, W.R., 1999. Global sea level rise and glacial isostatic adjustment. Glob. Planet. Change 20 (2–3), 93–123.

Piggot, J.D., 1995. A seismic classification scheme for clastic shelf wedges (deltas). In: Oti, M.N., Postma, G. (Eds.), Geology of Deltas. A.A. Balkema, Rotterdam, Netherlands, pp. 17–30.

Rampino, M.R., 1979. Holocene submergence of southern Long-Island, New-York. Nature 280 (5718), 132–134.

Schlager, W., 1993. Accommodation and supply — a dual control on stratigraphic sequences. Sediment. Geol. 86 (1–2), 111–136.

Siddall, M., Rohling, E.J., Almogi-Labin, A., Hemleben, C., Meischner, D., Schmelzer, I., Smeed, D.A., 2003. Sea-level fluctuations during the last glacial cycle. Nature 423 (6942), 853–858.

Stanley, D.J., Warne, A.G., 1994. Worldwide initiation of Holocene marine deltas by deceleration of sea-level rise. Science 265 (5169), 228–231.

Stuiver, M., Daddario, J.J., 1963. Submergence of the New Jersey Coast. Science 142, 451.

Stuiver, M., Polach, H.A., 1977. Reporting of C-14 data — discussion. Radiocarbon 19 (3), 355–363.

Stuiver, M., Reimer, P.J., 1993. Extended C-14 data-base and revised calib 3.0 C-14 age calibration program. Radiocarbon 35 (1), 215–230.

Tanabe, S., Hori, K., Saito, Y., Haruyama, S., Vu, V.P., Kitamura, A., 2003. Song Hong (Red River) delta evolution related to millennium-scale Holocene sea-level changes. Quat. Sci. Rev. 22 (21–22), 2345–2361.

Traykovski, P., Geyer, R., Sommerfield, C., 2004. Rapid sediment deposition and fine-scale strata formation in the Hudson estuary. J. Geophys. Res. Earth Surf. 109 (F2).

Uchupi, E., Driscoll, N., Ballard, R.D., Bolmer, S.T., 2001. Drainage of late Wisconsin glacial lakes and the morphology and late quaternary stratigraphy of the New Jersey–southern New England continental shelf and slope. Mar. Geol. 172 (1–2), 117–145.

Van de Plassche, O., 1990. Mid-holocene sea-level change on the eastern shore of Virginia. Mar. Geol. 91 (1–2), 149–154.

Van de Plassche, O., 1991. Late Holocene sea-level fluctuations on the shore of Connecticut inferred from transgressive and regressive overlap boundaries in salt-marsh deposits. J. Coast. Res. 159–179 (special issue no. 11).

Van de Plassche, O., Mook, W.G., Bloom, A.L., 1989. Submergence of coastal Connecticut 6000-3000 (C-14) years BP. Mar. Geol. 86 (4), 349–354.

Van de Plassche, O., van der Borg, K., de Jong, A.F.M., 2002. Relative sea-level rise across the Eastern Border fault (Branford, Connecticut): evidence against seismotectonic movements. Mar. Geol. 184 (1–2), 61–68.

Van der Wal, D., Pye, K., Neal, A., 2002. Long-term morphological change in the Ribble Estuary, northwest England. Mar. Geol. 189 (3–4), 249–266.

Weiss, D., 1974. Late Pleistocene stratigraphy and paleoecology of lower Hudson River Estuary. Geol. Soc. Amer. Bull. 85 (10), 1561–1570.

Willard, D.A., Cronin, T.M., Verardo, S., 2003. Late-Holocene climate and ecosystem history from Chesapeake Bay sediment cores, USA. Holocene 13 (2), 201–214.

Woodruff, J.D., Geyer, W.R., Sommerfield, C.K., Driscoll, N.W., 2001. Seasonal variation of sediment deposition in the Hudson River Estuary. Mar. Geol. 179, 105–119.

Worzel, J.L., Drake, C.L., 1959. Structure section across the Hudson River at Nyack, New York, from seismic observations. Ann. N.Y. Acad. Sci. 80, 1092–1105.

Zaitlin, B.A., Dalrymple, R.W., Boyd, R., 1994. The stratigraphic organization of incised-valley systems associated with relative sea-level change. In: Dalrymple, R.W., Boyd, R., Zaitlin, B.A. (Eds.), Incised-valley Systems: Origin and Sedimentary Sequences. SEPM (Society for Sedimentary Geology) Special Publication, vol. 51, pp. 45–60.

Please cite this article as: A.L. Slagle et al., Late-stage estuary infilling controlled by limited accommodation space in the Hudson River, Marine Geology (2006), doi:10.1016/j.margeo.2006.07.009.